

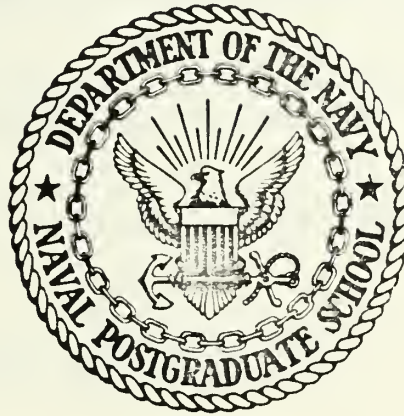
A STUDY OF THE EFFECT OF THE ION EX-  
CHANGE STRENGTHENING METHOD ON  
MACROFLAWS IN SODA-LIME GLASS

William Richard Burcham



# NAVAL POSTGRADUATE SCHOOL

## Monterey, California



# THESIS

A STUDY OF THE EFFECT OF THE ION EXCHANGE  
STRENGTHENING METHOD ON MACROFLAWS IN SODA-LIME GLASS

by

William Richard Burcham

Thesis Advisor:  
Co-Advisor:

J. J. von Schwind  
Robert B. Leonesio

MAR 1972

*Approved for public release; distribution unlimited.*



A Study of the Effect of the Ion Exchange  
Strengthening Method on Macroflaws in Soda-Lime Glass

by

William Richard Burcham  
Lieutenant, United States Navy  
B.S., Kansas State University, 1964

Submitted in partial fulfillment of the  
requirements for the degree of

MASTER OF SCIENCE IN OCEANOGRAPHY

from the

NAVAL POSTGRADUATE SCHOOL  
March 1972



## ABSTRACT

This work examines the strengthening effect of the ion exchange method of chemical tempering on two specific types of macroflaws, a thermally blunted crack and a sawcut, in soda-lime glass. The use of these macroflaws permitted a quantitative fracture mechanics analysis of the amount of strengthening produced, and a greater access for ion exchange at the flaw tip than could be afforded by a sharp crack. The specimens were treated for various lengths of time in a potassium nitrate bath at 365°C. A double cantilever cleavage technique of measuring fracture surface energy was used to find  $G_c$ , the strain energy release rate. The average increase in  $G_c$  was found to be roughly linear reaching a maximum level of approximately 200% at twelve hours of treatment for the blunted crack specimen type, while a similar maximum of approximately 200% was reached at six hours of treatment for the sawcut specimen type.





## TABLE OF CONTENTS

I.	INTRODUCTION .....	6
II.	PROPERTIES AND BEHAVIOR OF GLASS .....	7
III.	ION EXCHANGE STRENGTHENING .....	9
IV.	FRACTURE MECHANICS ANALYSIS .....	11
V.	EXPERIMENTAL PROCEDURE .....	14
VI.	RESULTS AND DISCUSSION .....	25
	A. SPECIMENS USED .....	25
	B. DISCUSSION OF SPECIMEN BEHAVIOR .....	26
	C. DATA PRESENTATION AND DISCUSSION .....	29
	D. RELATIONSHIP TO PREVIOUS WORKS .....	51
VII.	RECOMMENDED FURTHER STUDIES .....	53
VIII.	CONCLUSIONS .....	54
	LIST OF REFERENCES .....	55
	INITIAL DISTRIBUTION LIST .....	57
	FORM DD 1473 .....	58



## LIST OF TABLES

I.	Composition and Characteristics of the Glass Used .....	14
II.	Average $G_c$ 's and Standard Deviations for Type I Specimens..	34
III.	Maximum and Minimum $G_c$ 's for Type I Specimens .....	36
IV.	Average $G_c$ 's and Standard Deviations for Type II Specimens <sup>c</sup> .....	39
V.	Maximum and Minimum $G_c$ 's for Type II Specimens .....	40
VI.	Comparison of Various $G_c$ 's .....	44
VII.	$G_c$ 's of Special Type I Specimens .....	48
VIII.	Fracture Surface Energies of Soda-Lime Glass, Other Studies .....	52



## LIST OF FIGURES

1. Liemandt's Sharp Pre-Cracked Sample .....	13
2. Type I Sample Configuration .....	15
3. Type II Sample Configuration .....	16
4. Thermal Treatment Equipment .....	18
5. Specimen Cutting Apparatus .....	20
6. Polariscopes .....	21
7. Type I Macroflaw Within Guide Groove .....	21
8. Salt Bath Equipment .....	23
9. Fracture Testing Equipment .....	24
10. Illustration of Crack Healing .....	27
11. Type I Macroflaw Tip .....	28
12. Photoelastic Stress Patterns .....	30-31
13. Type I Specimen Fracture Mode .....	32
14. Type II Specimen Fracture Mode .....	33
15. $G_c$ vs Treatment Time Plot for All Type I Specimens .....	37
16. Average $G_c$ 's with Standard Deviations and Maximum $G_c$ 's vs Treatment <sup>C</sup> Time Plot for Type I Specimens .....	38
17. $G_c$ vs Treatment Time Plot for All Type II Specimens .....	41
18. Average $G_c$ 's with Standard Deviations and Maximum $G_c$ 's vs Treatment <sup>C</sup> Time Plot for Type II Specimen .....	42
19. $G_c$ 's of Sharp Pre-Cracked and Type I Specimens vs Zero Treatment Time .....	45
20. $G_c$ 's of Heat and Non-Heat Treated Type II Specimens vs Zero Treatment Time .....	46
21. Type I Specimen Used for Special Testing .....	47
22. $G_c$ 's vs Treatment Method of Special Type I Specimens .....	50



## I. INTRODUCTION

The physical properties of glass, transparency, hardness, moderate density as compared to steel, the ability to withstand great compressive loads, and the unique characteristic of being strengthened by the high pressures of the ocean depths rather than weakened as metals, have made it a prime candidate for underwater structural use. Further recommendations for its use are its relative low cost and ease of forming. Major disadvantages are its brittleness, the phenomenon of delayed fracture, and a lack of industrial capability adequate to the task of producing massive glass structures. Considerable work is being expended on the study of glass in an effort to improve its characteristics. This paper investigates the effect of one method of strengthening glass on a macroscopic flaw. A discussion of the properties and behavior of glass, including ion exchange strengthening and a fracture mechanics analysis, is given by Liemandt [1]. A brief review of these topics is presented here as a matter of convenience. A fracture mechanics approach to the mode of failure is used to provide a quantitative description of the strengthening effect.





## II. PROPERTIES AND BEHAVIOR OF GLASS

That glass is amorphous has been demonstrated by x-ray diffraction methods which show only broad spectrum patterns [2]. Thus, the state of glass is classified as vitreous, and is intermediate to the state of the usual solids which exhibit rigidity and the random structure of liquids. Most industrial glasses are silica ( $\text{SiO}_2$ ) based, and are characterized by a random distribution of interlocking silica tetrahedra,  $\text{SiO}_4$ . Covalent bonding of each  $\text{Si}^{++++}$  ion with 4  $\text{O}^{--}$  ions occurs with each  $\text{O}^{--}$  ion sharing electrons with 2  $\text{Si}^{++++}$  ions. Tables of ionic radii by Pauling [3] show that  $\text{Si}^{++++}$  has an ionic radius of 0.41Å and  $\text{O}^{--}$  has an ionic radius of 1.40Å. Oxide additives such as  $\text{Na}_2\text{O}$ ,  $\text{Al}_2\text{O}_3$ , etc., are present in most glass and create an excess of  $\text{O}^{--}$  ions. This excess encourages the presence of mechanical weakness in the material. Thus, glasses are a random network of  $\text{SiO}_4$  tetrahedra with metallic and alkali ions interspersed throughout.

The fictive temperature of glass is defined as that temperature above which the rate of internal structural changes are great enough to produce a state of equilibrium with the temperature, and below which structural changes are so slow as to be negligible. In production, as the glass melt cools to the fictive temperature, each ion is locked into a network which conforms to its ionic shape. Any further diffusion is over high potential barriers. A cavity formed by diffusion of an ion is filled by another diffusing ion to preserve electroneutrality.

Glass is a brittle material which follows Hooke's Law during loading to failure. The length of the zone of plastic deformation is on the order of one atomic bonding distance [4].



The compressive strength of glass is so great that catastrophic failure is generally due to tensile stress [5]. The random atomic structure and brittleness of glass make it very vulnerable to surface flaws where a tensile stress may be generated by a compressive load and become concentrated. Factors which affect the observed strengths include the rate and type of loading and the temperature and medium in which the tests are conducted.

A method of strengthening glass is to produce a compressive stress in its surface layers. This compressive stress must be overcome before a tensile stress can develop to a magnitude required for failure. Methods for producing a surface compressive stress include thermal tempering, coating with a glass characterized by a lower coefficient of expansion while the specimen is being shaped, creation of a layer with a low coefficient of expansion by crystallization, and ion exchange at the surface. The last method is the one used for this investigation and will be discussed in more detail.



### III. ION EXCHANGE STRENGTHENING

Ion exchange strengthening consists of exchanging larger alkali metal ions for smaller alkali metal ions in the surface layer of a glass article. This is accomplished by placing the glass which contains a small alkali metal ion in its network in a molten salt containing a larger alkali metal ion. Ion exchange is a diffusion process caused by a concentration gradient between the different ions. It is dependent upon the temperature, time of treatment, and the relative concentrations of the ions in question.

The ions of interest in this experiment were the sodium<sup>I</sup> in the glass and the potassium<sup>I</sup> of the salt bath. Pauling's calculated diameter for the sodium<sup>I</sup> ion is 1.90A, and 2.66A for the potassium<sup>I</sup> ion [3]. A compressive stress is induced in the surface which is proportional to the size differential of the two ions exchanged. The large ion stretches the silicon-oxygen bonds between silica tetrahedra in the glass network surrounding the transfer location. Using Stookey's [6] formula for surface stress

$$S_c = \frac{1}{3} \frac{E}{1-\mu} \cdot \frac{\Delta V}{V} \quad (1)$$

where  $S_c$  is the surface stress,  $E$  is Young's modulus,  $\mu$  is Poisson's ratio, and  $v$  is the volume of the surface layer, it can be shown that a theoretical compressive stress of 210,000 psi will result from a sodium<sup>I</sup>-potassium<sup>I</sup> exchange in a glass having a Young's modulus of  $10^7$  psi.



Griffith in 1920 [7] showed that failure originates at surface flaws due to the extremely high stress concentrations at their tips. These flaws can be so small as to be unobservable even by microscopic methods. The mere touching of pristine glass was found to drastically reduce its strength. A quantitative description of these high stress concentrations can be obtained using the formula of Hillig and Charles [8]. The maximum tensile stress near a flaw tip is given by

$$\sigma_m = 1 + 2S_t \sqrt{L/\rho} \quad (2)$$

Here  $S_t$  is the applied tensile stress,  $L$  is the flaw depth, and  $\rho$  is the radius of curvature at the crack tip.

The improvement in strength resulting from the ion exchange method of strengthening then results from the generated compressive layer reaching a sufficient depth to counteract the effect of Griffith microflaws. The application of this strength mechanism to macroflaws in this work permitted the use of a fracture mechanics analysis to describe the quantitative increase of strength for a specific flaw.





#### IV. FRACTURE MECHANICS ANALYSIS

In this study double-cantilever specimens were used to measure the fracture energy of soda-lime glass before and after treatment in a potassium nitrate bath. This technique was originally developed by Gilman [9], modified by Westwood and Hitch [10], extensively utilized by Wiederhorn [11, 12, 13, 14, 15, 16], and more recently by Liemandt [1].

The magnitude of the stress field at a crack tip may be expressed in terms of a single parameter  $K$ , the stress intensity factor, which is a function of the applied load and the crack dimensions. When a critical stress field exists at the crack tip, that is,  $K = K_C$ , where  $K_C$  is the fracture toughness, failure occurs due to rapid crack propagation. The fracture toughness is a constant for any given material and is related to another parameter  $G$ , the strain energy release rate [16]. The functional relationship between  $G$  and  $K$  is given by

$$G = \frac{K^2}{E} (1-\mu^2) \quad \text{for plane strain} \quad (3a)$$

$$G = \frac{K^2}{E} \quad \text{for plane stress} \quad (3b)$$

The strain energy release rate is a measure of the energy per unit area available for the crack extension process.

There exists a critical strain energy release rate,  $G_C$ , which is the sum of the surface energy and the energy absorbed by plastic deformation at the crack tip. It occurs when  $K$  is equal to  $K_C$ . Thus

$$G_C = 2\gamma + U \quad (4)$$

where  $\gamma$  is the surface energy of the material (factor of two required due to generation of two surfaces) and  $U$  is the plastic deformation energy.



The small size of the plastic deformation zone in glass [4] (the basic reason for the material's brittleness) implies a negligibly small plastic deformation energy  $U$ . Equation (4) then becomes

$$G_c \doteq 2\gamma . \quad (5)$$

The brittle nature of glass requires that the relationship of the critical strain energy release rate,  $G_c$ , and the fracture toughness,  $K_c$ , should be that of plane strain, as given by Equation (3a).

The double cantilever beam technique for measuring fracture surface energies requires only that the force necessary to propagate a crack be known in addition to the specimen dimensions. The sharp, pre-cracked sample configuration of Liemandt is shown in Figure 1. For this arrangement the surface energy of the material is given by

$$\gamma = \frac{6P^2L^2}{Ewb^3t^3} [1 + 1.34t/L + 0.45(t/L)^2] \quad (6)$$

where  $P$ ,  $L$ ,  $w$ ,  $b$ ,  $t$  are the applied force, crack length, and specimen dimensions, respectively, as shown in Figure 1.  $E$  is again Young's modulus [16]. This equation was determined to be valid for crack lengths greater than approximately 1.5 times  $t$ , the specimen half height.

Specimen modification for the present work was minor. The minor alterations and the desire to demonstrate the relative effect of the ion exchange method of strengthening of glass permitted the utilization of Equation (6) without further modification.

The value of fracture toughness can be altered by environmental effects such as temperature and humidity [13]. Efforts were taken to minimize environmental effects such as stress corrosion wheresoever possible.



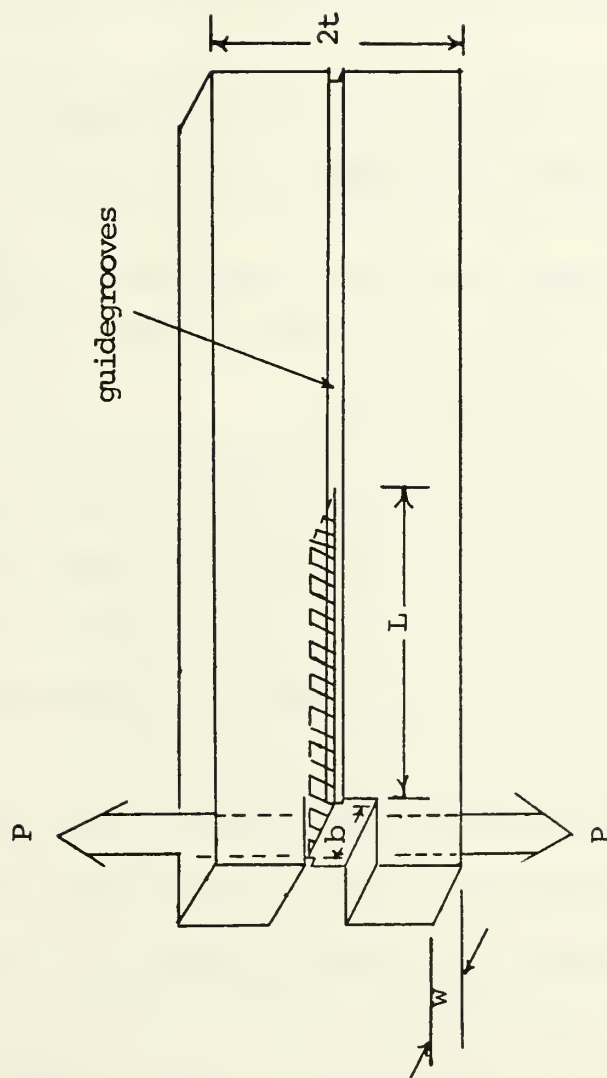


Figure 1. Liemandt's Sharp Pre-Cracked Sample.  
 $P$  is the applied force,  $L$  is the crack length,  
 $2t$  and  $w$  are the specimen outside dimensions,  
and  $b$  is the specimen width between grooves.



## V. EXPERIMENTAL PROCEDURE

The specimens used in this experiment were cut from sheets of PPG Industries, Inc., Pennvernon<sup>®</sup> soda-lime glass. Its composition and characteristics are given in Table I. The glass and specimen types were picked to provide direct comparison with the earlier work of Liemandt [1].

Table I. Composition and Characteristics of the Glass Used

Glass 3/16" Soda-Lime Sheet	Composition (weight percent)						
	SiO <sub>2</sub>	Na <sub>2</sub> O	CaO	MgO	Na <sub>2</sub> SO <sub>4</sub>	Fe <sub>2</sub> O <sub>3</sub>	Al <sub>2</sub> O <sub>3</sub>
	73%	13.25%	8.2%	3.55%	0.21%	0.11%	1.2%
plus traces of NaCl and K <sub>2</sub> O							
Young's Modulus .....							10 <sup>7</sup> psi
Poisson's Ratio .....							0.22
Strain Point Temperature .....							521°C
Annealling Temperature Range .....							516-575°C

The samples used here were slightly modified forms of Liemandt's design and are shown in Figures 2 and 3. The modifications consist of the substitution of a thermally blunted open macroflaw for the sharp, closed macroflaw of the Liemandt sample thus producing Specimen Type I, and a blunt sawcut to produce Specimen Type II. The open macroflaws were chosen to provide greater access to the flaw tip to facilitate the ion exchange operation.





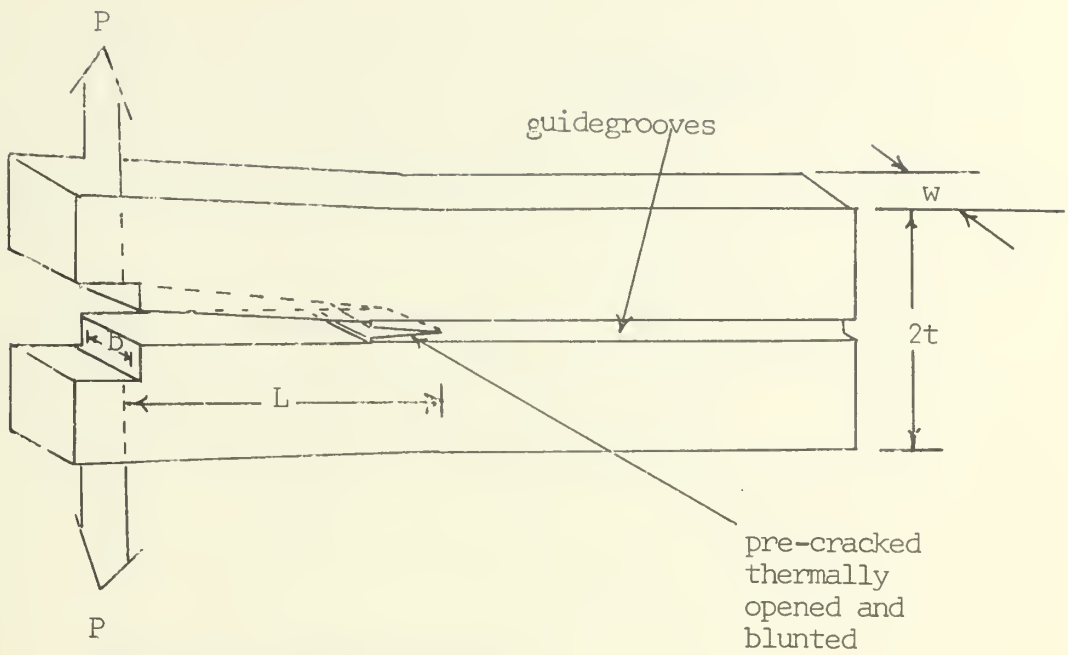


Figure 2a. Specimen Type I

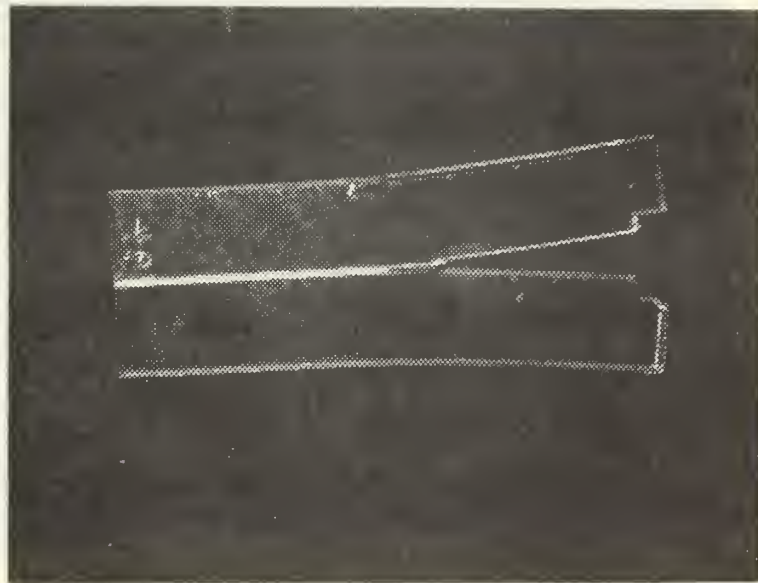


Figure 2b. Specimen Type I  
 $P$  is the applied force,  $L$ , is the crack length,  
 $b$  is the specimen thickness between guide grooves,  
and  $2t$  and  $w$  are the outside dimensions.



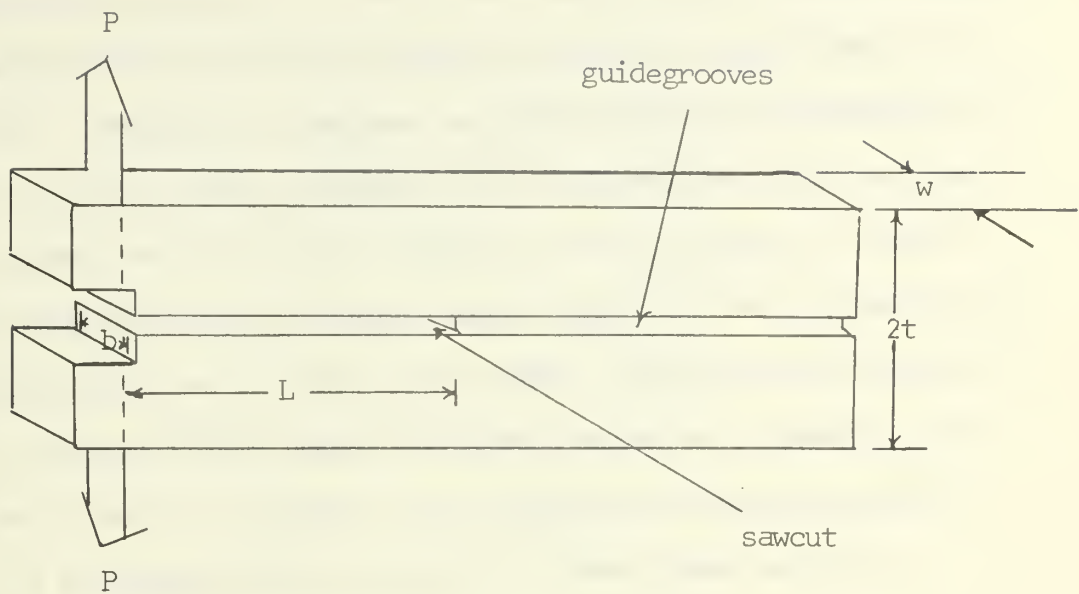


Figure 3a. Specimen Type II

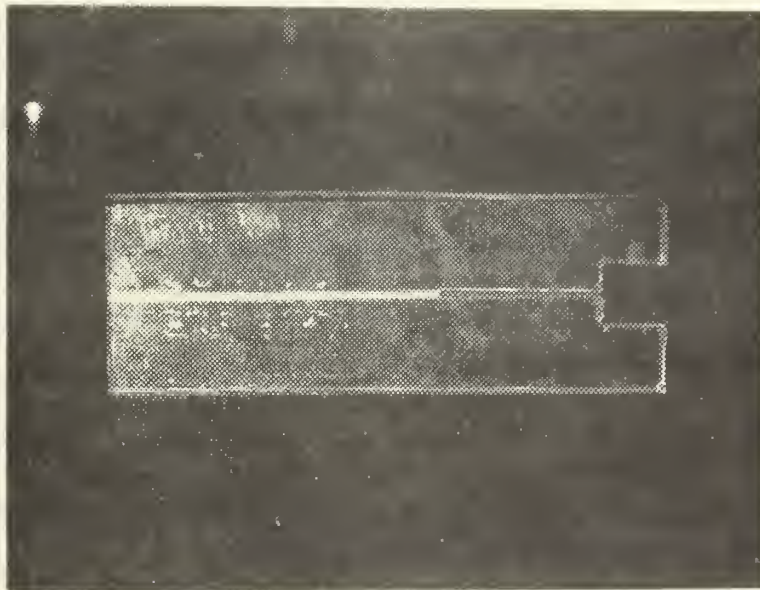


Figure 3b. Specimen Type II  
 $P$  is the applied force,  $L$  is the crack length,  
 $b$  is the specimen thickness between guide  
 grooves, and  $2t$  and  $w$  are the outside dimensions.



The specimens were cut to roughly one inch by three inch rectangles with a loading notch ground in one end to a depth of approximately one quarter inch. The Type I specimens were then notched longitudinally to a depth of one inch using a diamond saw. Small scribe marks were made with a tungston carbide scribe at the tip of the saw notch. A small crack was then initiated by thermal shock induced by the application of a small soldering iron to these scribe marks. The crack was then led a distance of one-half inch beyond the sawcut using the soldering iron. All cracks of the Type I samples were immediately contaminated with graphite in a molybdenumdisulfide base to retard crack healing, a phenomenon which will be discussed in the section on results. The molybdenumdisulfide evaporated rapidly leaving a graphite residue. It is believed that the graphite residue within the crack physically held the crack open thus partially retarding crack healing.

The macroflaws of the Type I specimens were opened and thermally blunted in a standard glass blower's oven. The specimens were placed side by side, horizontally in a rack and loaded with a three-quarter pound weight during heat treatment. The apparatus used is shown in Figure 4. The complete heat treatment cycle of twelve hours was automatically controlled. The oven was brought to a temperature of  $610^{\circ}\text{C}$ , approximately the softening temperature of the glass, in a period of four hours. The specimens were returned to room temperature at a controlled rate of cooling for the next eight hours. This process served to anneal the samples and in this manner all Type I specimens were standardized to a common starting point. All flaw lengths of the Type I specimens were roughly 3t.





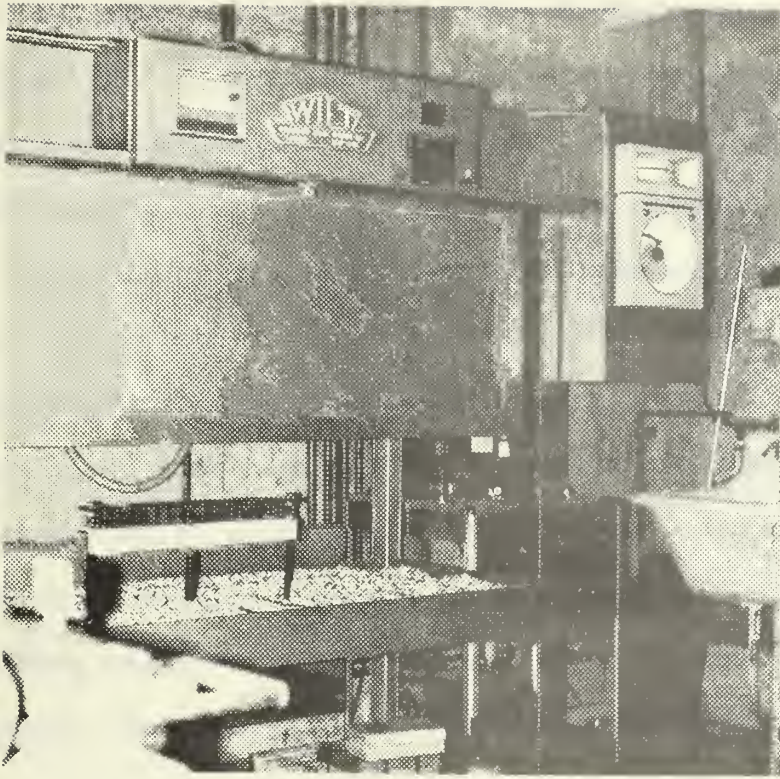
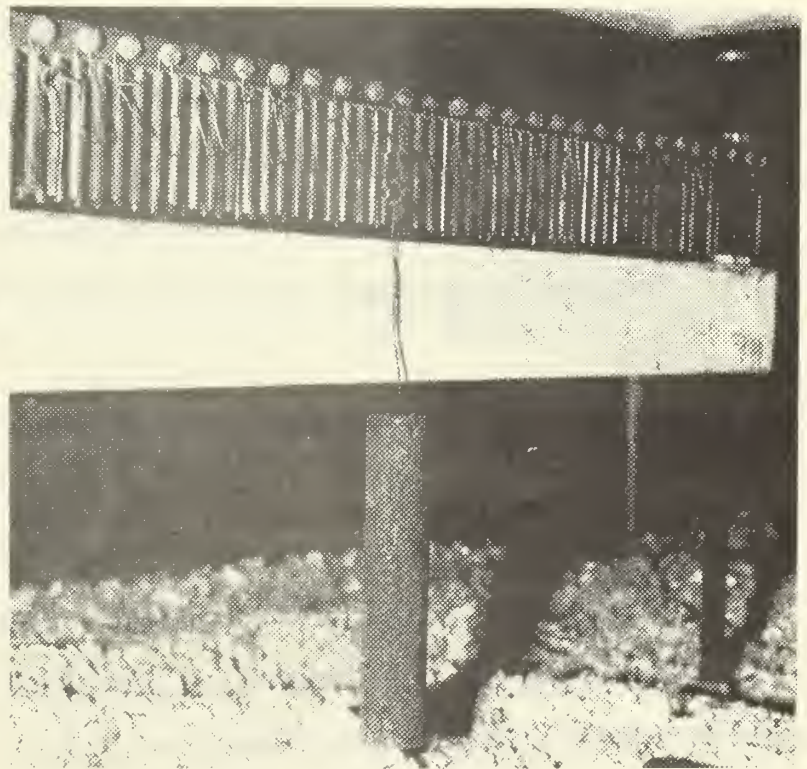


Figure 4a.  
Glass Blowers Oven  
Used in Heat Treatment  
of Specimens

Figure 4b.  
Specimen in Holding  
Rack with Weight  
Attached to Specimen  
as During Thermal  
Blunting Operation







The sawcut macroflaw of the Type II specimens and the guide grooves utilized on both specimen types were formed using the diamond saw and fixture shown in Figure 5. The Type II specimen sawcut macroflaws were approximately  $2.5t$  where  $2t$  again was the specimen height.

The guide grooves which were 0.26" wide and approximately 0.25" deep were used on both sample types as the best method to keep the crack, generated at failure, centered and nearly parallel to the specimen sides. The guide grooves also provided a means of compensating for the phenomenon of crack healing which occurred in the Type I samples. The grooves were applied to the Type I samples after annealing. Polariscopic examination of these samples after the application of the grooves, utilizing the equipment shown in Figure 6, disclosed no significant residual stress. The orientation of a typical thermally blunted macroflaw within a guide groove is shown in Figure 7.

Guide grooves were applied to the Type II specimens prior to annealing. The Type II specimens were subjected to a heat treatment identical to that of the Type I specimens except that no weights were utilized during heat treatment as the sawcut required no further opening. Polariscopic examination of all Type II samples after annealing disclosed no residual stresses.

Several of each type of specimen were fractured after the above fabrications to act as standards for the remainder of the investigation.

In order to facilitate comparison the ion exchange treatment of the samples was identical to that performed by Liemandt [1]. A brief description of the sample treatment is provided here for convenience. The specimens were immersed in a  $\text{KNO}_3$  salt bath held at  $365^\circ\text{C} \pm 5^\circ\text{C}$  for varying lengths of time. All macroflaws were examined prior to submergence in and



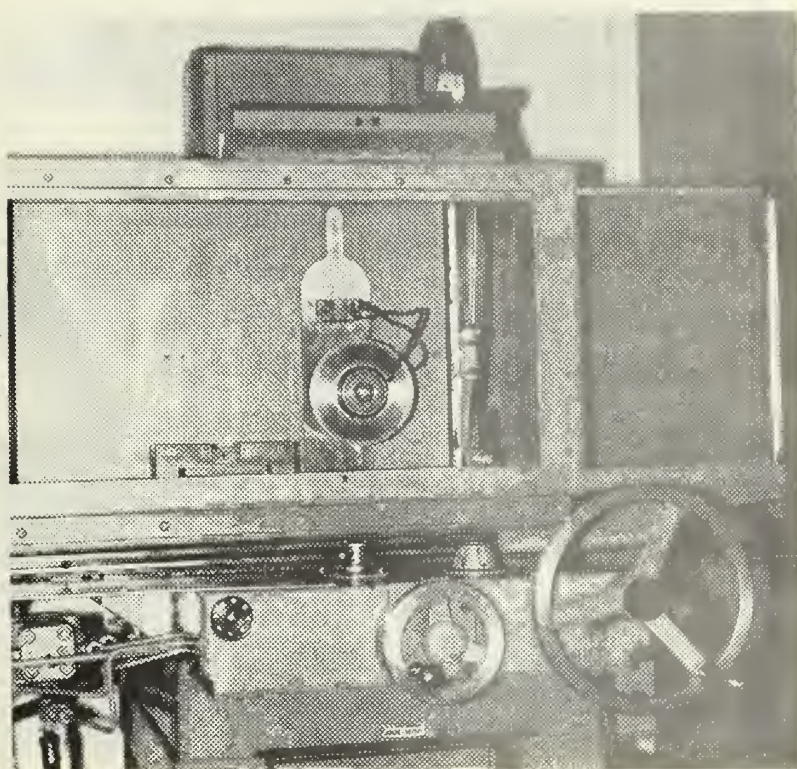
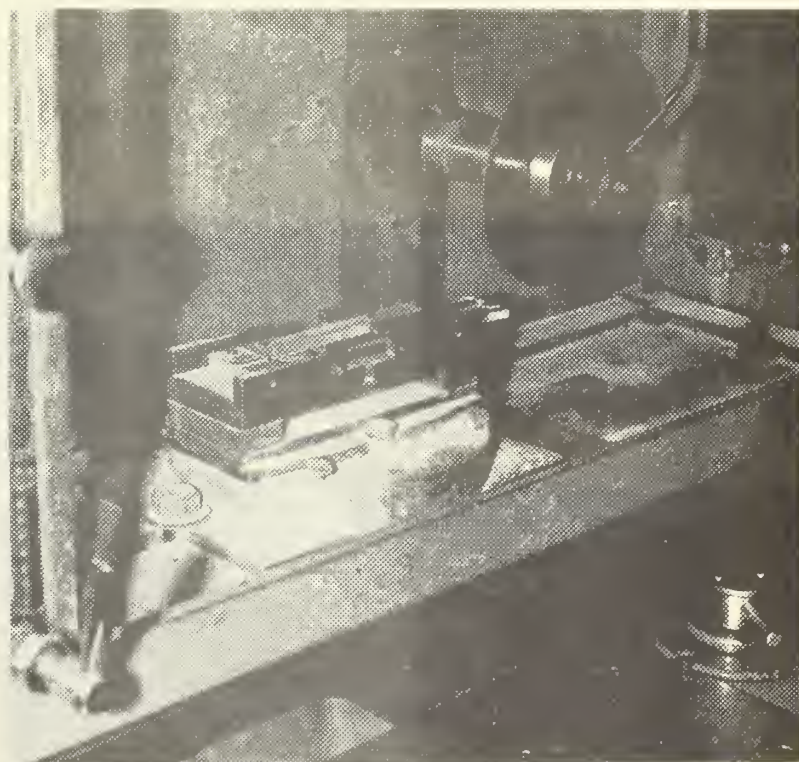


Figure 5a.  
The Diamond Saw Used  
to Produce Guide  
Grooves and Macroflaws  
is Shown

Figure 5b.  
Sample Holding Fixture  
Used with the Diamond  
Saw to Produce Sawcut  
Macroflaws and Guide  
Grooves is Shown







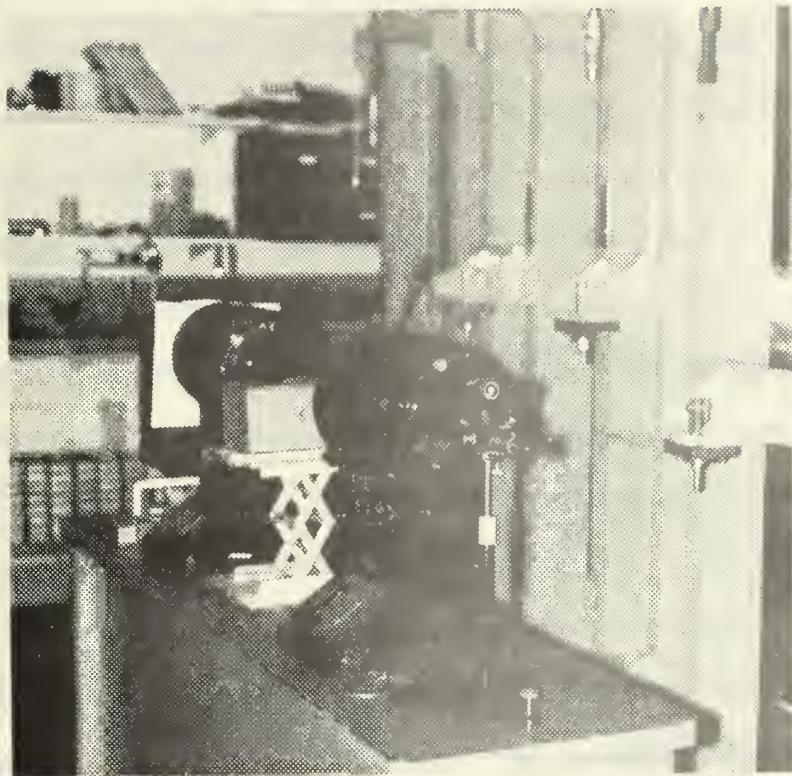


Figure 6.  
Polariscope Used to  
Examine Residual Stress  
in the Specimens

Figure 7.  
Orientation of a  
Typical Type I  
Macroflaw Within  
a Guide Groove





after removal from the salt bath to check for any extension or healing. The salt bath used during this experiment is shown in Figure 8. All specimens were slowly lowered via a pulley arrangement through a ten gallon can which served as a warming compartment. The lowering and raising took place over periods of one hour and 40 minutes respectively to minimize thermal shock. C-clamps were used to create slight compressive stress fields at the macroflaw tips upon removal from the warming chamber. The specimens were then immersed in water until all solidified salt dissolved. This procedure was introduced by Liemandt [1] to prevent stress corrosion cracking of the specimens. Very few samples were lost to this phenomenon while utilizing this technique. After treatment the specimens were loaded to failure on an Instron testing machine utilizing the fixtures shown in Figure 9. The recessed edges of the fixtures act as approximate knife edge loading points within the loading notches of the specimens. The Instron testing machine was calibrated to ten pound loads prior to each testing session. The crosshead speed was maintained at .05 inches per minute. Typical loading times to failure were less than four seconds.

Prior to ion exchange treatment, measurements of the crack length, and specimen height were made using a Gaertner traveling microscope. Specimen thickness and the thickness between the grooves were measured using a Mitutoyo dial caliper. The traveling microscope provided measurements of  $\pm .0001$  in. The dial caliper provided measurements of  $\pm .001$  in.





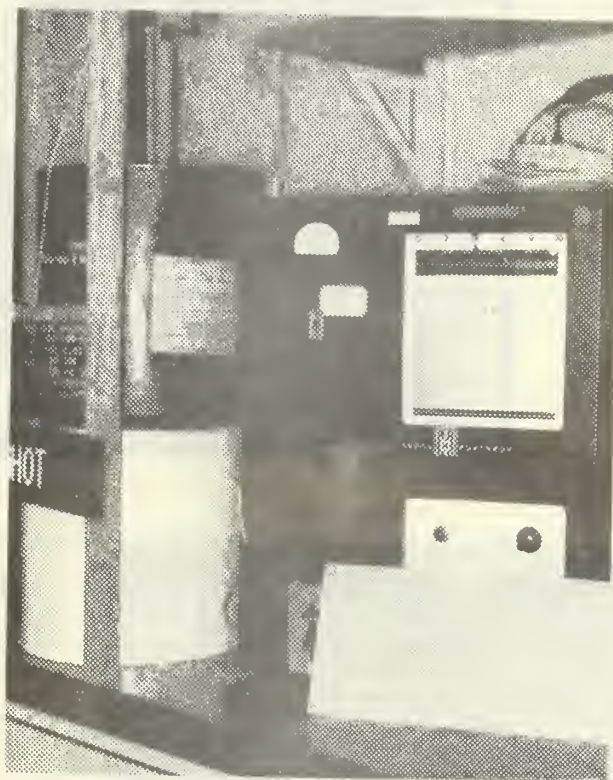


Figure 8. The ten gallon can which served as the warming and cooling compartment is shown over the salt bath. The temperature control unit is in the right foreground.



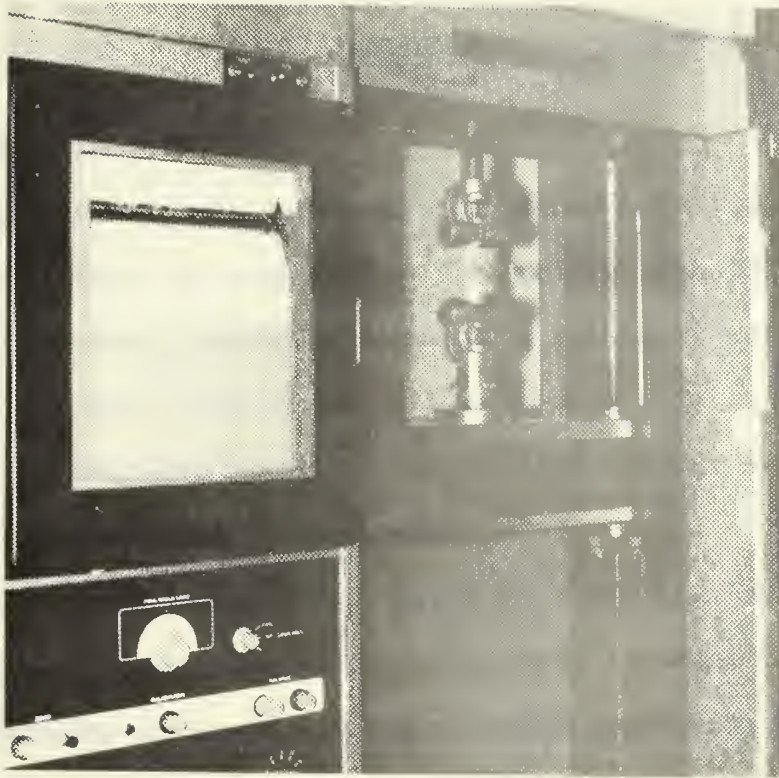
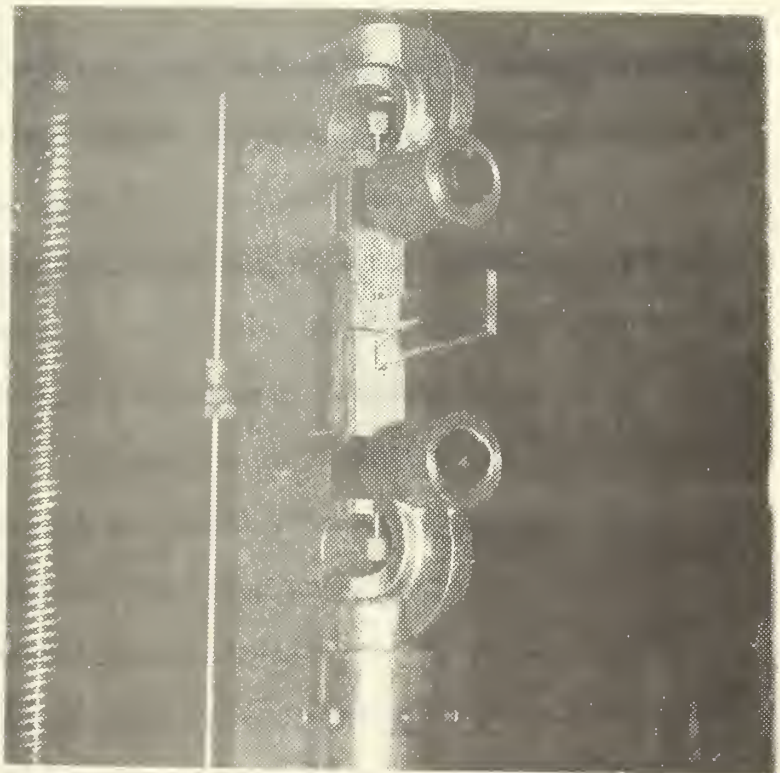


Figure 9a.  
The Specimens Were  
Tested to Failure  
Upon This Instron  
Machine

Figure 9b.  
Specimen is Shown  
Held in Fixtures  
Used During Testing  
to Failure





## VI. RESULTS AND DISCUSSION

### A. SPECIMENS USED

Approximately 440 specimens were prepared for use in the experiment. Of this number, 105 were used as data points, and the balance in development of standard production techniques, initial experimenting, were broken, or were rejected for various reasons to be described. A large number of specimens was discarded when the Instron testing machine was found to be incorrectly calibrated.

Even though the specimen design and production techniques were essentially those utilized or developed by Liemandt [1], modification of the specimens increased individual sample production time to approximately one hour and fifteen minutes per sample. This time was exclusive of the ion exchange treatment time.

Of the 105 data points actually used, 8 were Type I, thermo-blunted, specimens fractured prior to any ion exchange treatment to establish a control strain energy release rate for the glass used. One group of 8 Type II, sawcut, specimens was fractured similarly to establish control for that part of the experiment in which that sample type was used and to provide correlation with the Type I specimens. Another group of 8 Type II specimens was fractured prior to annealing to establish the effect of this phase in the production method. Eight Liemandt specimens, sharp pre-cracked, were manufactured and fractured prior to any ion exchange to provide direct correlation with his experiment. The macroflow tips of ten Type I specimens were coated with an impermeable cement prior to ion exchange treatment. Four of these were subsequently fractured after treatment of one-half hour. The remainder were fractured after treatment





of 24 hours. This was done to establish the manner of ion diffusion into the macroflaw. Six Type I specimens were treated for 24 hours prior to the application of guide grooves to demonstrate the surface nature of the strengthening phenomenon. Finally, 57 specimens were treated by the ion exchange method for various periods of time to determine its strengthening effect. All specimens which underwent the ion exchange treatment did so in a  $\text{KNO}_3$  bath held at  $365^\circ\text{C}$ .

#### B. DISCUSSION OF SPECIMEN BEHAVIOR

During the production of the Type I specimens apparent crack healing was noted in all specimens. Two examples of this phenomenon are shown in Figure 10. The healing occurred prior to and during the heat treatment stage of production of the Type I samples. It is believed that the displacement of the new crack surfaces generated by the thermal shock technique was insufficient to prevent realignment and healing of a percentage of the bonds broken [19]. Immediate contamination of the newly formed cracks with graphite in a molybdenumdisulfide base (commercial name Lubri-Bond "A") retarded but did not completely eliminate the healing.

Much of the healed material which remained after heat treatment of the contaminated cracks was eliminated when the guide grooves were applied to the specimens. This is shown schematically in Figure 11. The healing took place most readily at the outside edges of the cracks and progressed along and into the cracks simultaneously, thus producing a macroflaw with a crescent shaped tip. The application of the guide grooves physically removed most of the healed material leaving two small regions whose dimensions averaged .015" along the specimen edges by .02" into the specimen centers. The Type I specimens were standardized in this manner.





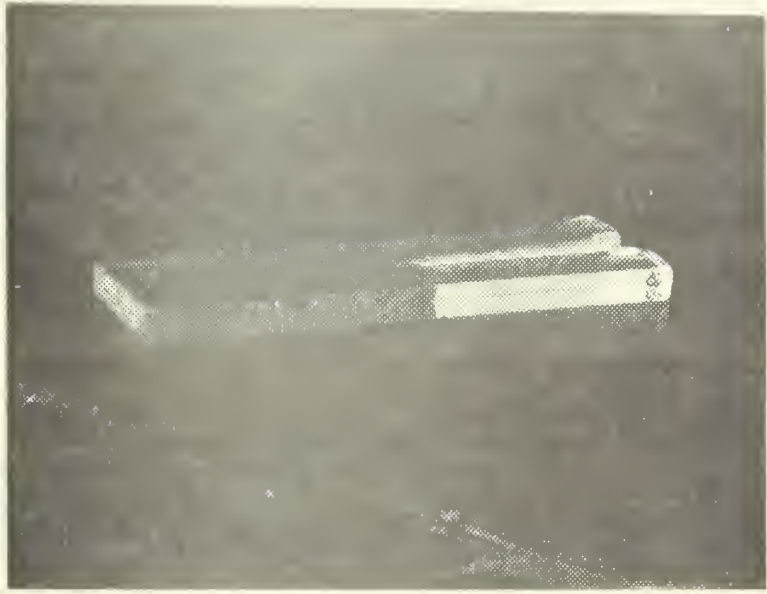


Figure 10a. Type I specimen showing reduced crack with rounded edges resulting from crack healing.

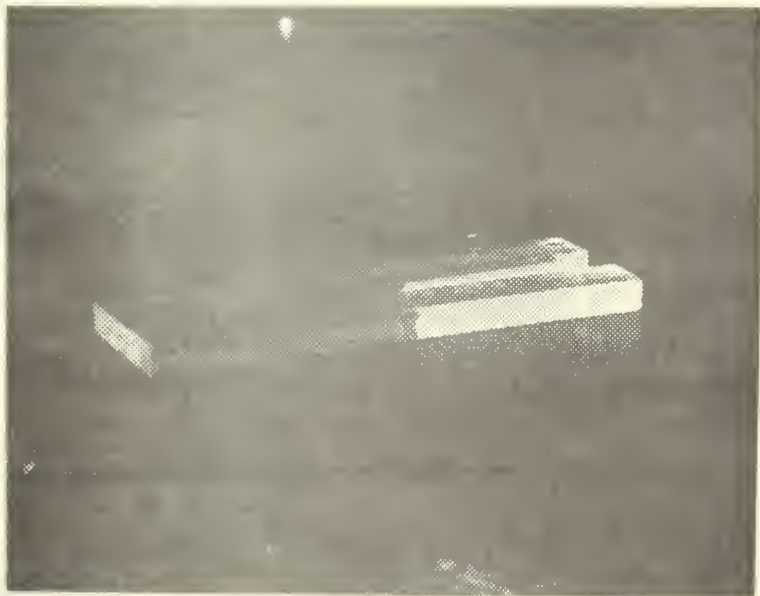


Figure 10b. Type I specimen showing apparent total crack healing.



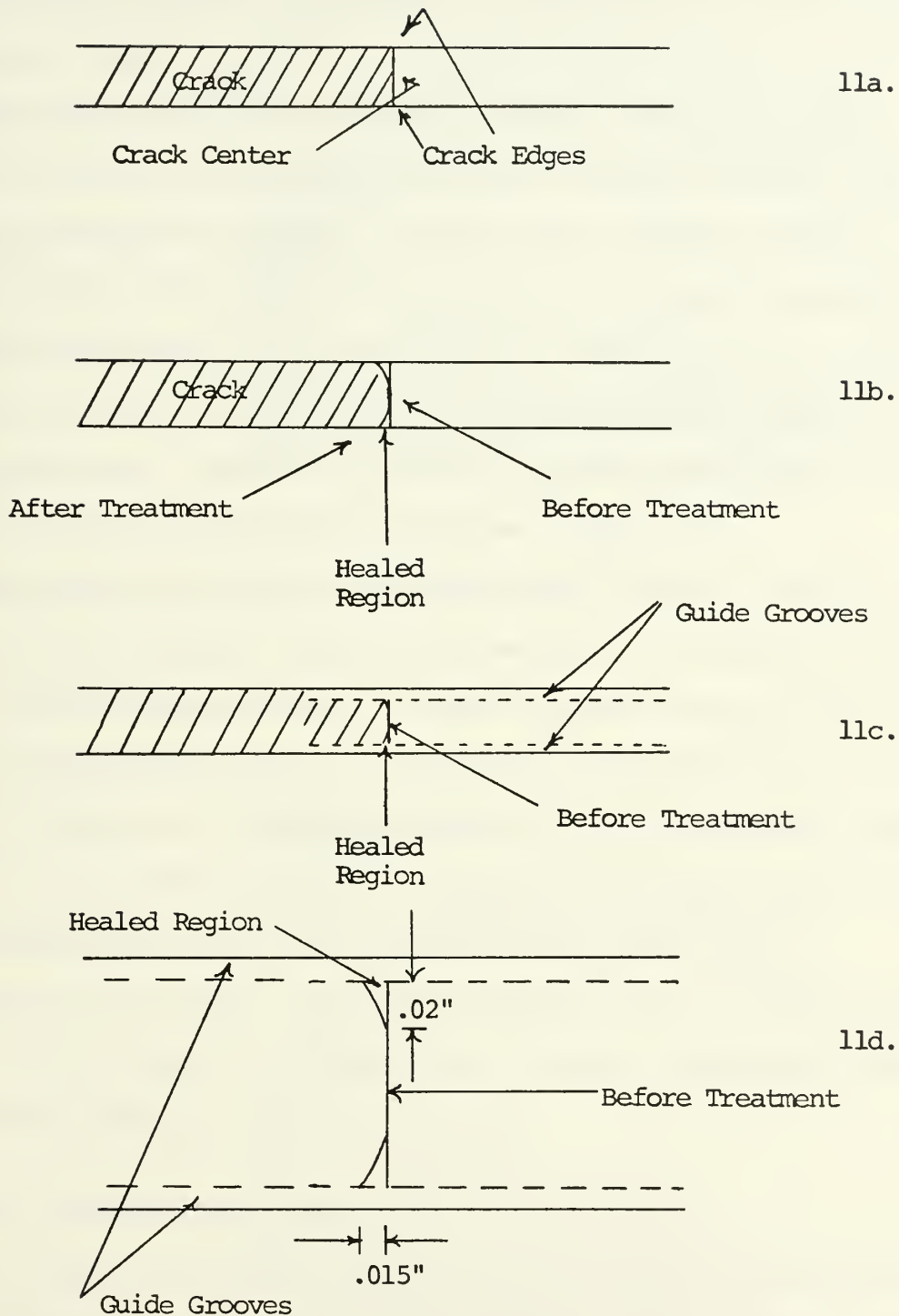


Figure 11. Figure 11a shows the crack edge and center upon initial production. Figure 11b shows the crack tip formed by crack healing. Figure 11c illustrates the removal of most of the healed region by application of guide grooves to the specimen. Figure 11d shows the magnitude of the average residual healed areas in accepted specimens.



Healing was not a problem in the Type II specimens as the surfaces of the macroflaws produced by the sawcut were physically separated by a distance of .026".

After being cut into the one inch by three inch size specimens and prior to further production steps, the glass exhibited residual stress when polariscopically examined. Following heat treatment, however, the Type I specimens with guide grooves as well as the Type II specimens appeared to be free of any residual stress. Both sample types exhibited evidence of residual stress under the polariscope after treatment in the ion exchange bath. Examples of the stress patterns exhibited at varying stages of production and testing are shown in Figure 12.

The majority of the Type I specimens tested fractured within the guide grooves along the entire length of the specimen. The remainder of the Type I specimens fractured with the crack following the guide grooves for a small distance then curving out to the edge of the specimen. These two modes of failure are illustrated in Figure 13. As this work was concerned with the force needed to initially generate two new crack surfaces, the data gathered from both of these modes of failure were used.

Only one of the Type II specimens fractured within the guide grooves along the entire length of the specimen. All other immediately broke out of the guide grooves as shown in Figure 14.

### C. DATA PRESENTATION AND DISCUSSION

The average critical strain energy release rates,  $G_c$ 's, accompanied by the standard deviations are listed in Table II for the Type I specimens. The rate of strengthening appears rapid to the 12 hour sample time. It then continues to generally increase, but at a reduced rate, to the termination of the experiment. The maximum and minimum  $G_c$ 's of the Type I



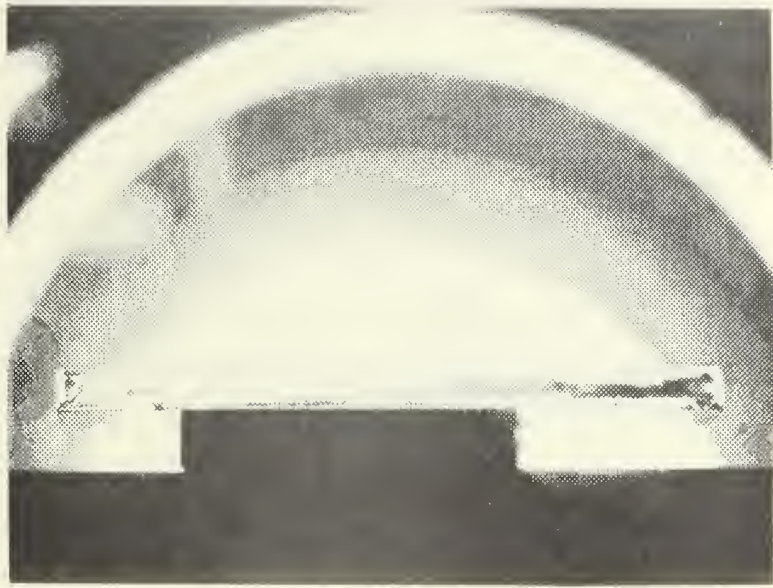


Figure 12a. The residual stress contained in the 1" x 3" specimens before annealing is shown.

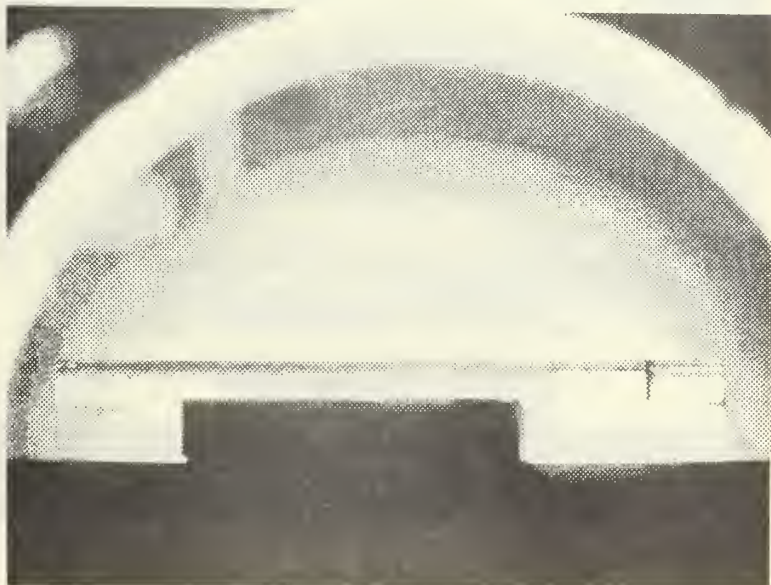


Figure 12b. A Type I specimen after heat treatment appears free of residual stress.







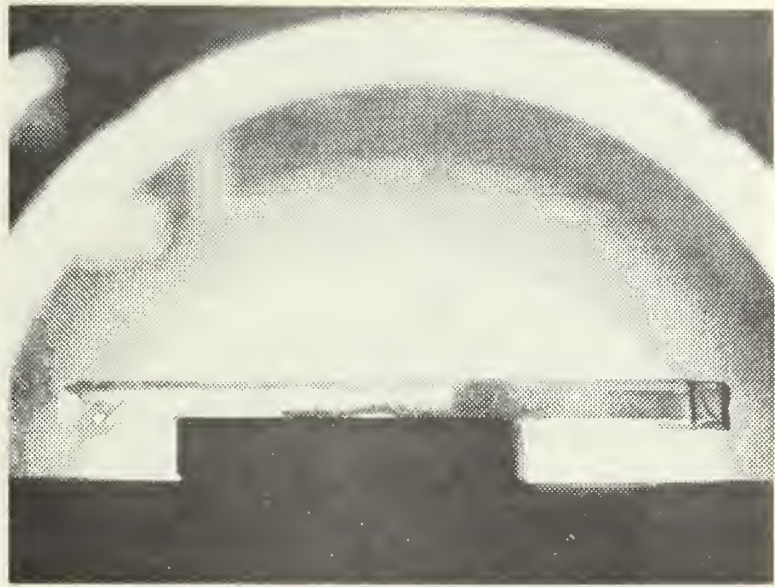


Figure 12c. Evidence of the compressive stress developed by treatment in the ion exchange bath for 60 hours is shown

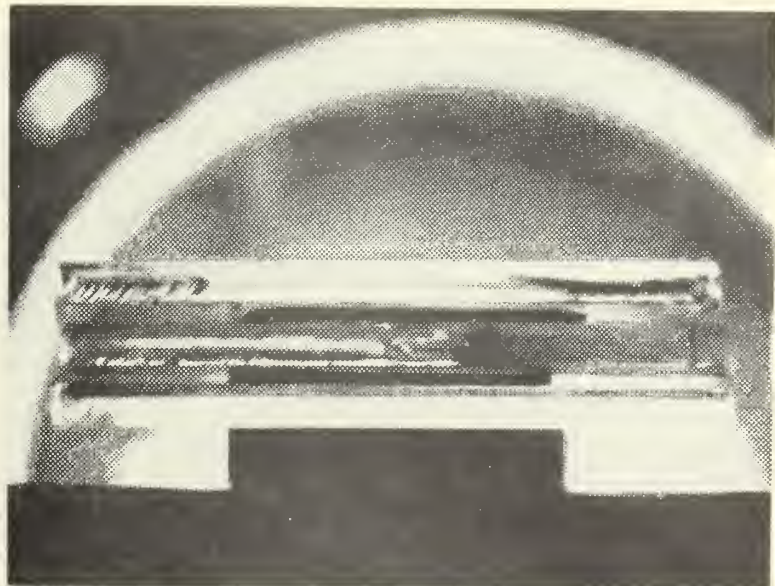


Figure 12d. The three previous samples are shown together for comparison. Top to bottom: As cut, 60 hour treatment, heat treated.



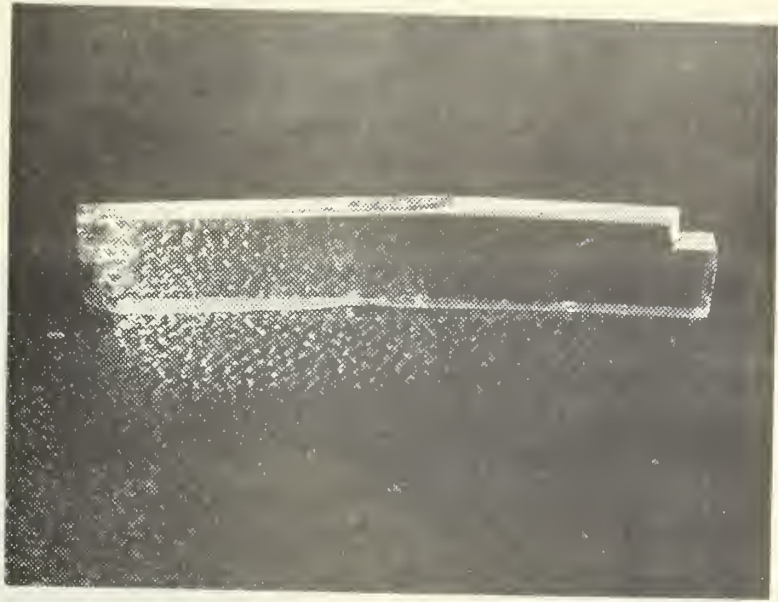


Figure 13a. Most of the Type I specimens fractured in the manner shown.

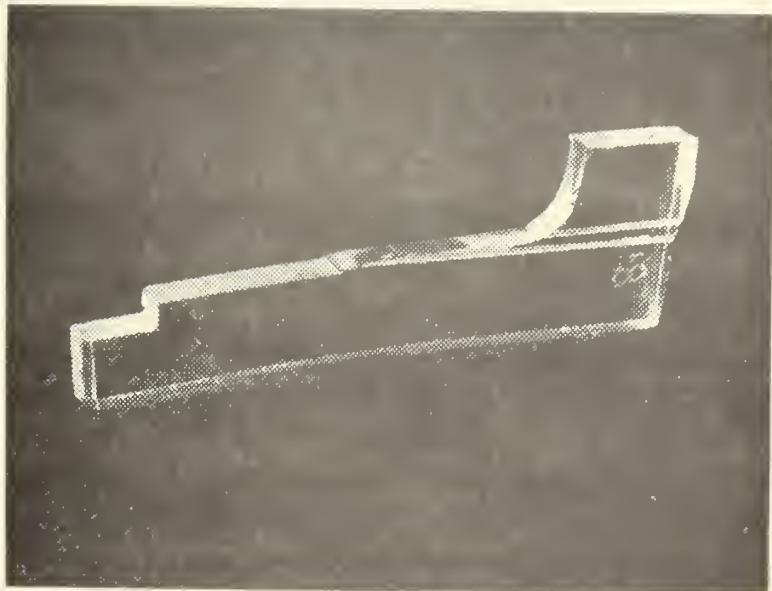


Figure 13b. The remainder of the Type I specimens fractured in the manner shown.



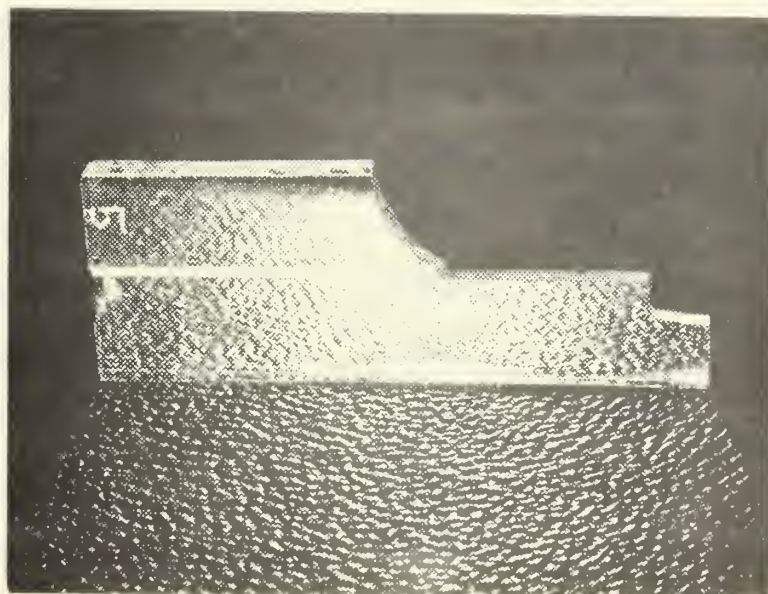


Figure 14. With the exception of one, all of the Type II specimens fractured as shown.



Table II. Average  $G_c$  and Standard Deviations

Type of Specimen	Treatment Time	Number of Specimens	Average $G_c$ in-lbf/in <sup>2</sup>	Standard Deviation
I	Control	8	0.0221	0.0090
	6 hours	7	0.0281	0.0144
	12 hours	7	0.0392	0.0155
	18 hours	8	0.0363	0.0150
	24 hours	7	0.0357	0.0189
	36 hours	4	0.0400	0.0181
	48 hours	4	0.0459	0.0234
	60 hours	3	0.0425	0.0217
	72 hours	4	0.0493	0.0231





specimens are given in Table III and roughly reflect the pattern of the average  $G_C$  values. The values of all the  $G_C$ 's of the Type I specimens are plotted versus treatment time in Figure 15. The maximum  $G_C$ 's and the average  $G_C$ 's with their standard deviations are shown plotted versus treatment time in Figure 16.

The average  $G_C$ 's with standard deviations for the Type II specimens are listed in Table IV. (Type II specimens were cut with the saw and then annealed.) Table V lists the maximum and minimum values obtained. The strengthening rate is seen to be more rapid than that experienced by the Type I specimens. An apparent slowing or leveling off occurs after only six hours of treatment, and a decrease in strengthening is noted after eighteen hours. The increased strengthening rate is felt to result from the increased molten  $KNO_3$  flow within the sawcut macroflaw due to its larger physical dimensions. The decrease in strengthening noted at the 18 hour treatment time may be due to relaxation of the compressive stress in the glass surface due to a combination of the stress magnitude, treatment time, and treatment temperature [5]. The apparent increase in the value of the control  $G_C$  over that for the Type I specimens is due to the application of Equation (6) without consideration for the physical alteration of the specimens or the mode of failure, which occurred outside the guide grooves in the thicker material. Taking these factors into consideration, allowing  $b$  to equal  $w$  and  $t$  to equal the half-height to the sawcut edge, yields an average  $G_C$  of 0.0215, which agrees very closely with that of the Type I specimens. The strain energy release rates of the Type II specimens are presented plotted versus treatment time in Figure 17. The corresponding maximum  $G_C$ 's and average  $G_C$ 's with standard deviations are similarly shown in Figure 18.



Table III. Maximum and Minimum  $G_c$

Type of Specimen	Treatment Time	Number of Specimens	Maximum $G_c$ in-lbf/in <sup>2</sup>	Minimum $G_c$ in-lbf/in <sup>2</sup>
I	Control	8	0.0317	0.0160
	6 hours	7	0.0490	0.0140
	72 hours	7	0.0605	0.0311
	18 hours	8	0.0507	0.0229
	24 hours	7	0.0470	0.0282
	36 hours	4	0.0439	0.0360
	48 hours	4	0.0633	0.0280
	60 hours	3	0.0496	0.0369
	72 hours	4	0.0617	0.0400



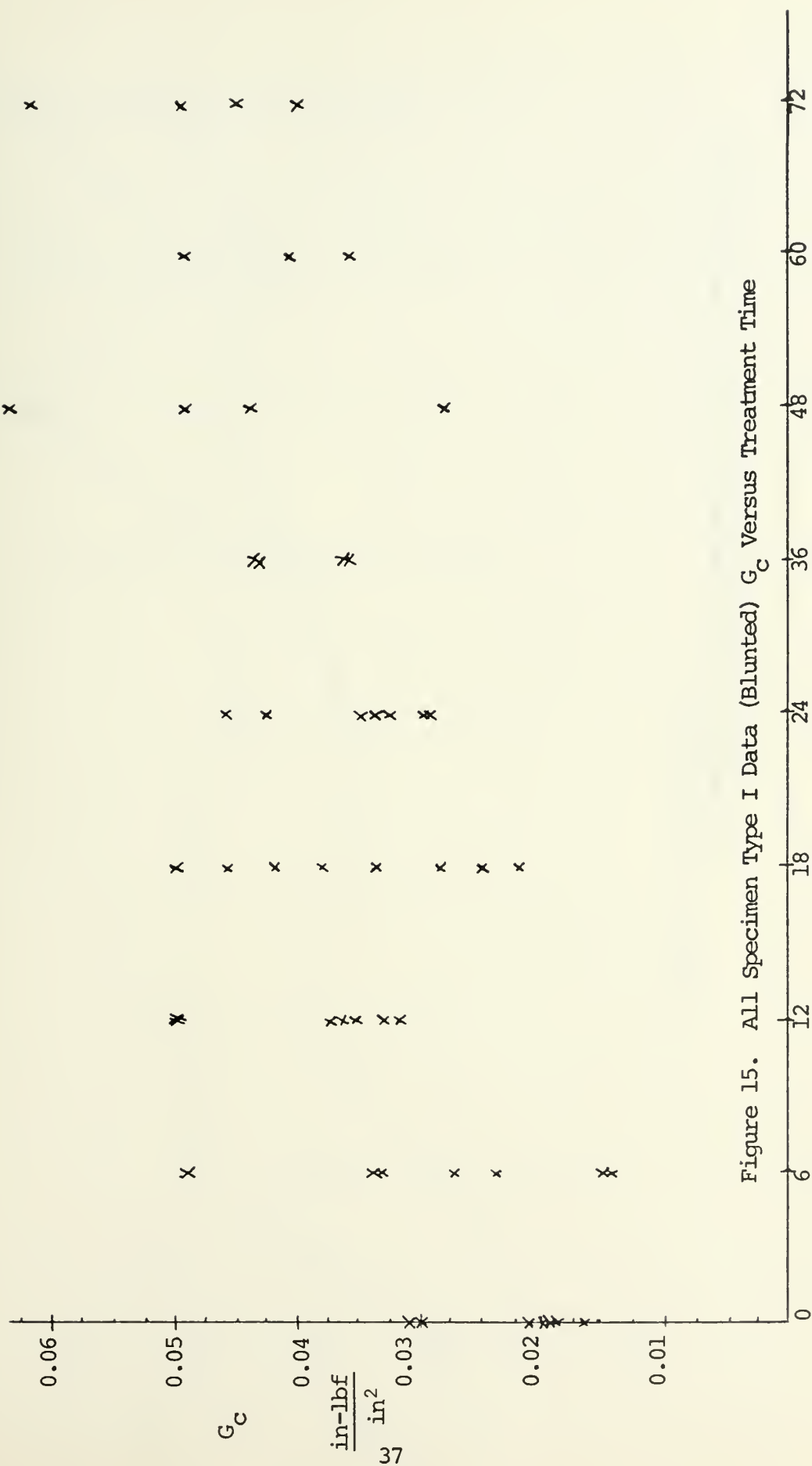


Figure 15. All Specimen Type I Data (Blunted)  $G_c$  Versus Treatment Time

Length of Treatment Time - Hours



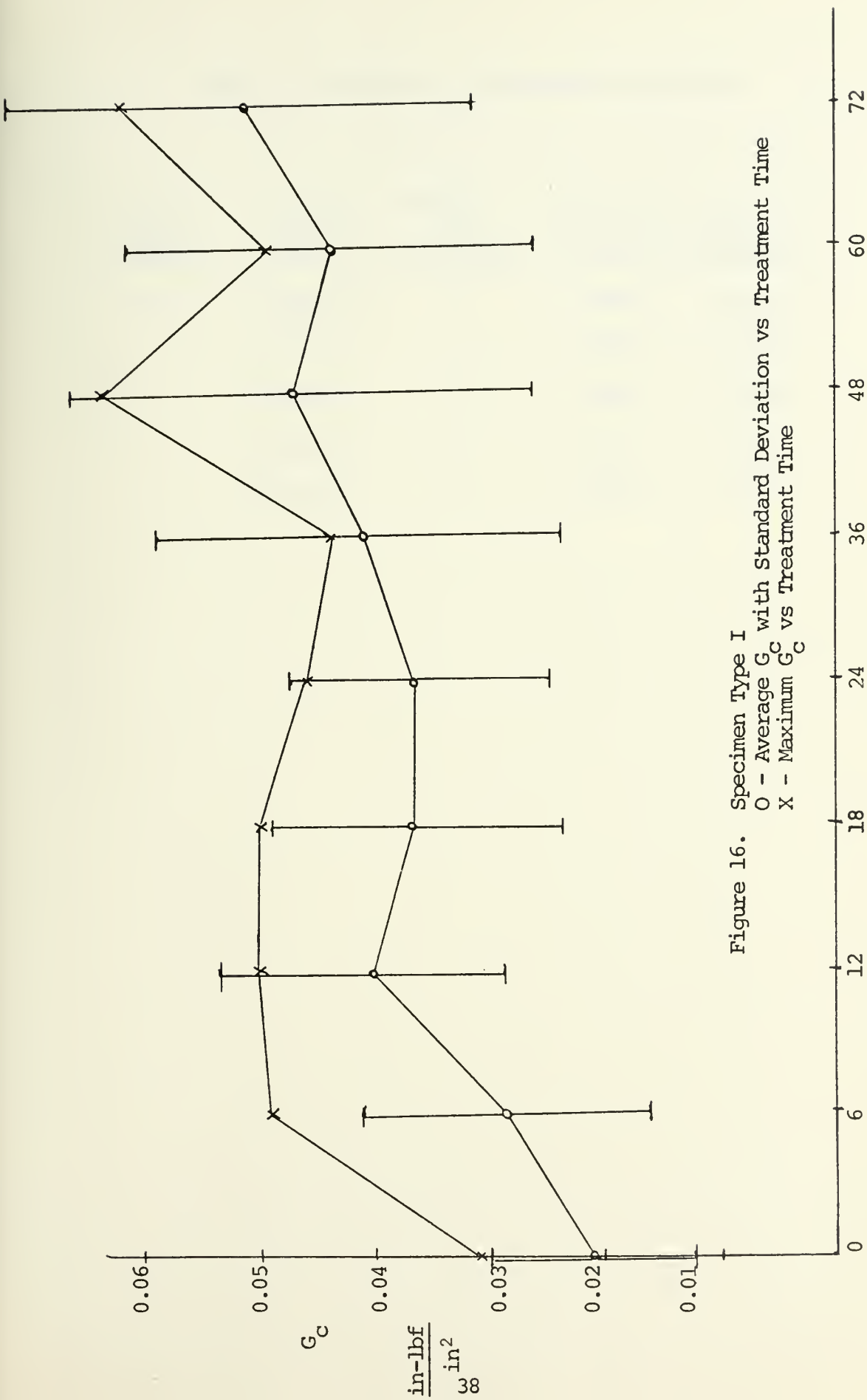


Figure 16. Specimen Type I  
 O - Average  $G_c$  with Standard Deviation vs Treatment Time  
 X - Maximum  $G_c$  vs Treatment Time

Length of Treatment Time - Hours





Table IV. Average  $G_c$  and Standard Deviations

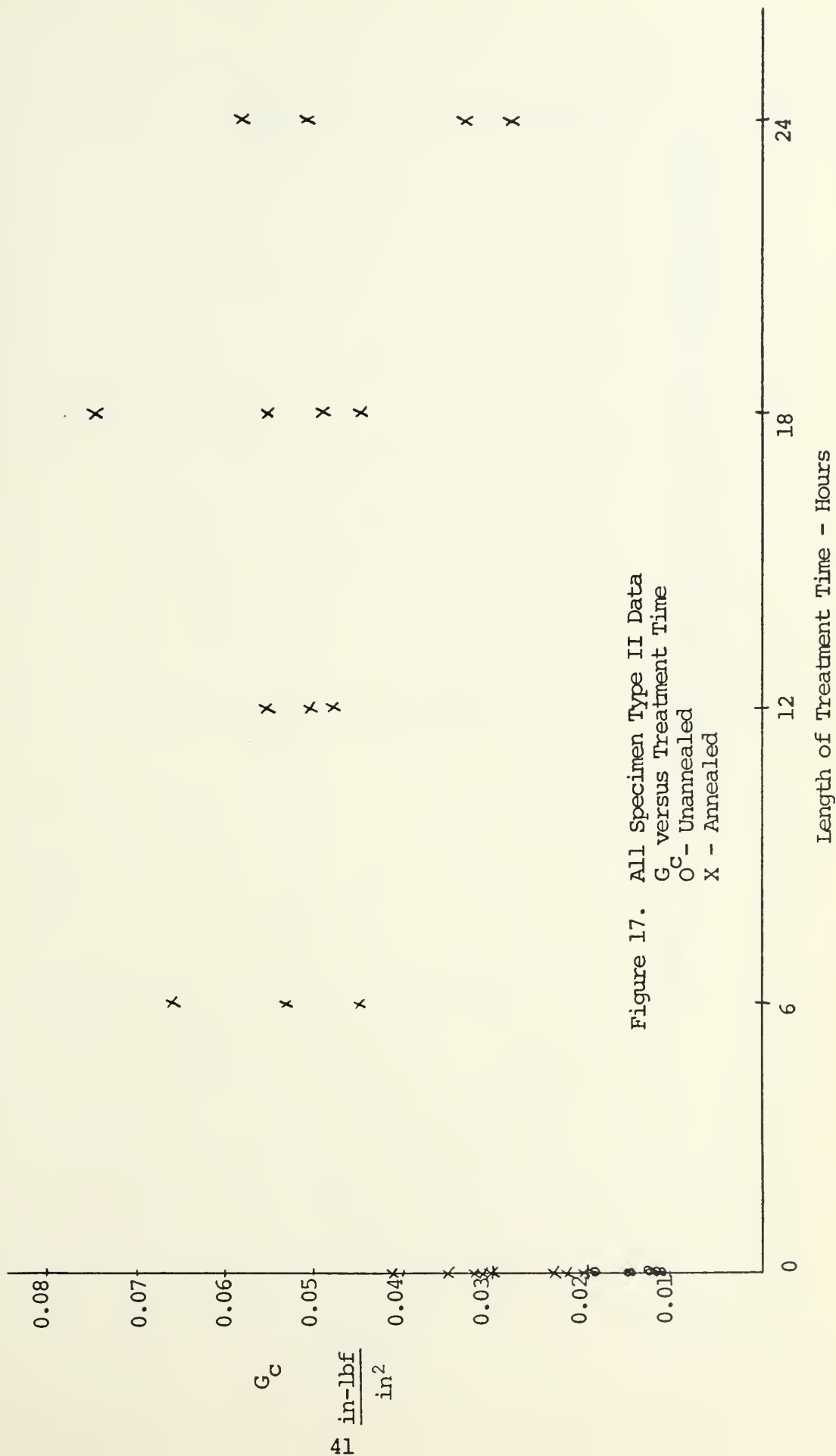
Type of Specimen	Treatment Time	Number of Specimens	Average $G_c$ in-lbf/in <sup>2</sup>	Standard Deviation
II	Control	8	0.0296	0.0117
	6 hours	3	0.0548	0.0283
	12 hours	3	0.0513	0.0258
	18 hours	4	0.0571	0.0276
	24 hours	4	0.0428	0.0219



Table V. Maximum and Minimum  $G_C$

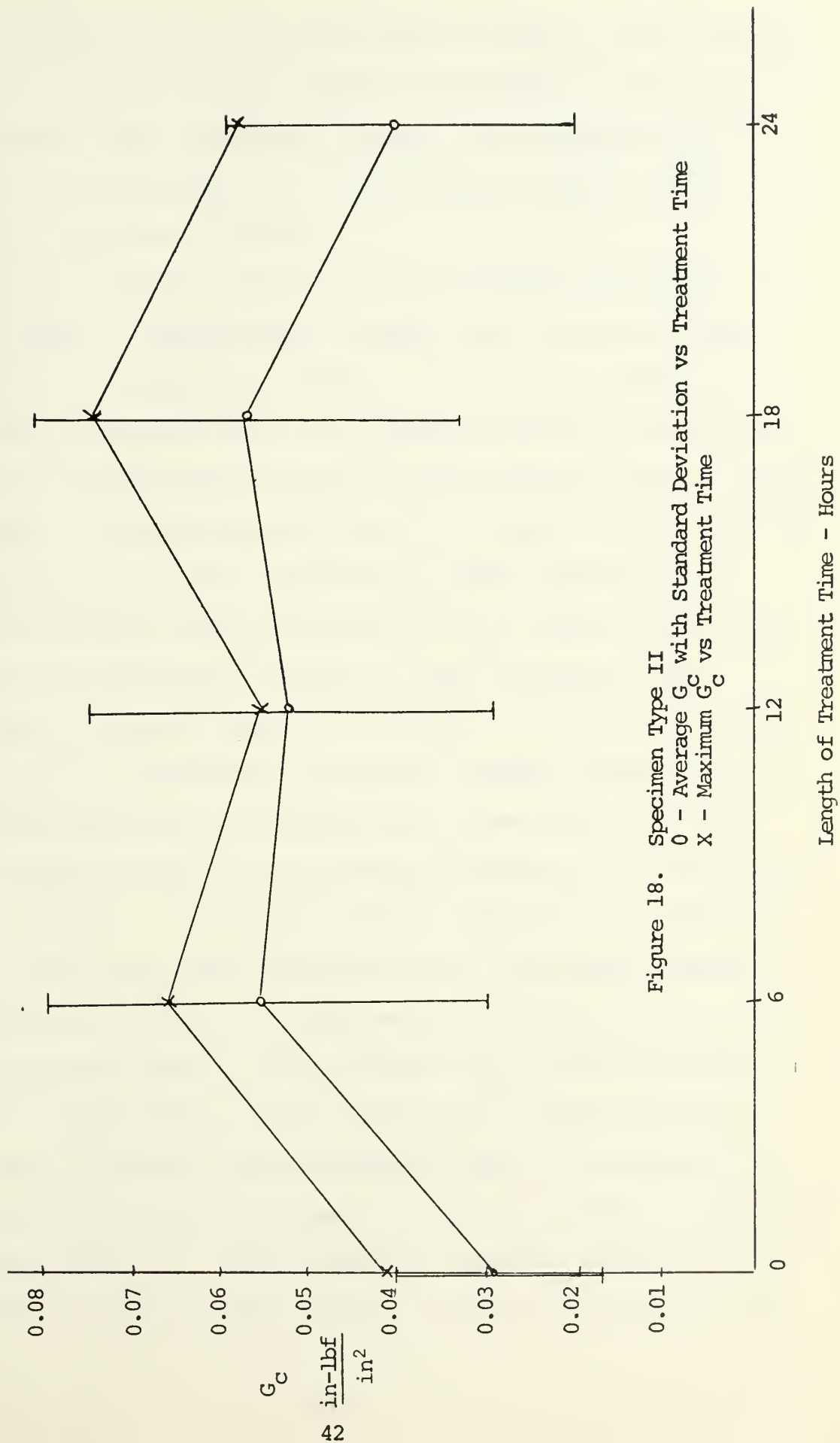
Type of Specimen	Treatment Time	Number of Specimens	Maximum $G_C$ in-lbf/in <sup>2</sup>	Minimum $G_C$ in-lbf/in <sup>2</sup>
II	Control	8	0.0412	0.0201
	6 hours	3	0.0658	0.0455
	12 hours	3	0.0551	0.0470
	18 hours	4	0.0754	0.0447
	24 hours	4	0.0592	0.0293













There appears to be no correlation between Liemandt's numeric results and those of this investigation. However, the production and fracture of eight Liemandt, sharp pre-cracked, specimens yielded values which did present a close relationship. It is felt that the values of  $G_C$  and  $K_C$  published by Liemandt are in error.

The maximum, minimum, and average  $G_C$ 's of the sharp pre-cracked specimens are compared to those of Type I control, Type II non-heat-treated, and Type II control specimens in Table VI. The sharp pre-cracked and Type I control specimens differ only in thermo blunting of the macroflaw. The Type II non-heat-treated and Type II control specimens share a similar relationship. As has been shown, the Type I and Type II control specimens are in reasonable agreement. The effect of thermal blunting is the difference between the sharp pre-cracked and Type I control specimens or the Type II non-heat-treated and Type II control specimens. These differences are presented graphically in Figures 19 and 20 respectively.

The tips of the macroflaws of ten Type I specimens were coated on their outside edges with an impermeable cement (see Figure 21). Four samples received one-half hour ion exchange treatments, the remaining six, 24 hour treatments. Additionally, six Type I specimens were treated for 24 hours prior to application of guide grooves. The average, maximum, and minimum  $G_C$ 's resulting from these tests are given in Table VII. All cement was removed from the coated specimens prior to fracture testing. Comparison of the average  $G_C$  for the one-half hour treated specimens to the average for the Type I control specimens reveals the contribution to the strengthening effect by the cement is negligible. The coated specimens which were treated for 24 hours exhibited an average  $G_C$  which was 88% of that of the uncoated specimens similarly treated. The average  $G_C$  of the



Table VI. Comparison of Various  $G_c$

Type of Specimen	Average $G_c$ in-lbf/in <sup>2</sup>	Maximum $G_c$ in-lbf/in <sup>2</sup>	Minimum $G_c$ in-lbf/in <sup>2</sup>
Sharp Pre-Cracked	0.0155	0.0189	0.0131
Type I Control	0.0221	0.0317	0.0160
Type II Non-heat Treated	0.0140	0.0191	0.0113
Type II Control	0.0296	0.0412	0.0201



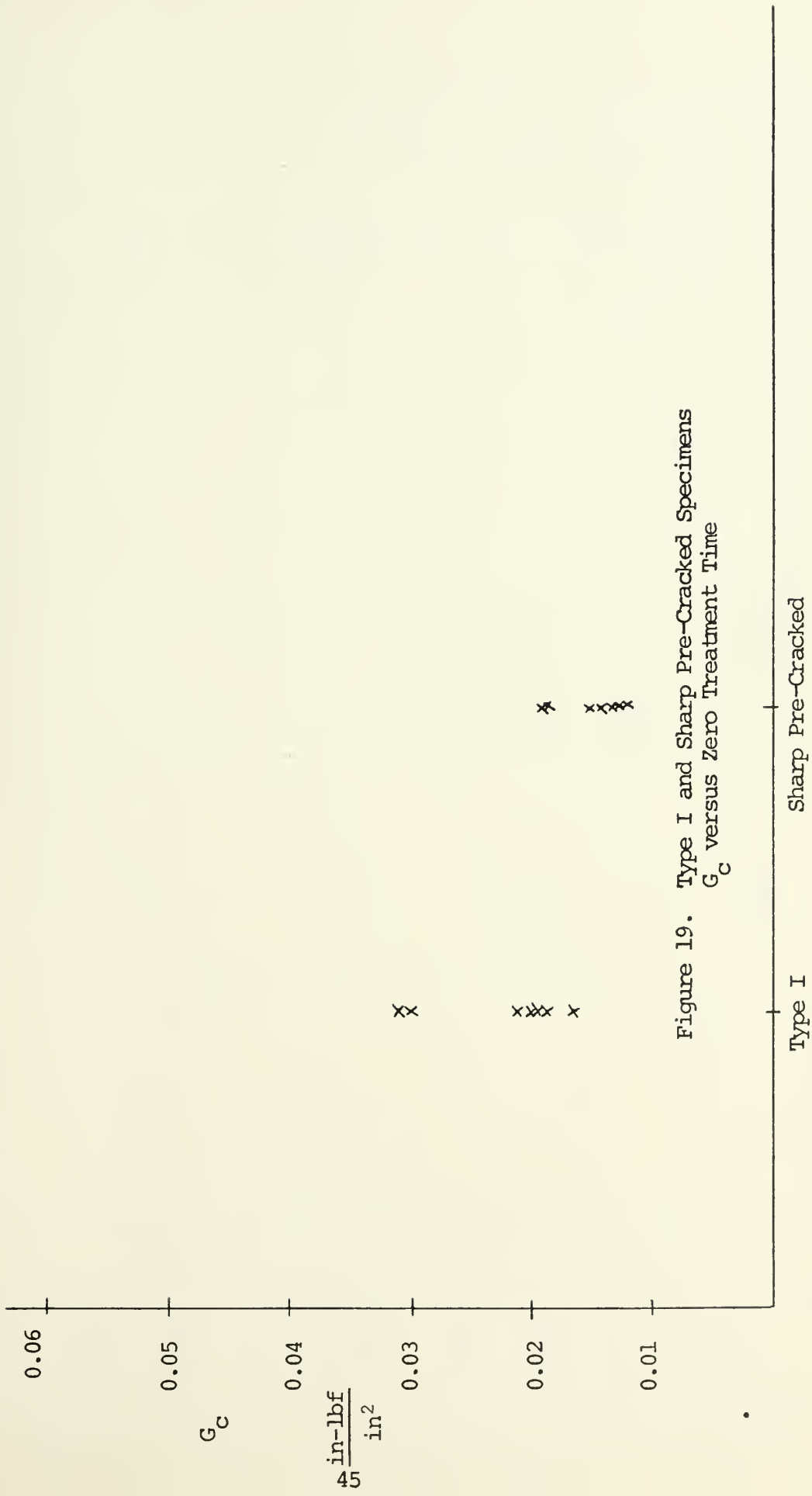


Figure 19. Type I and Sharp Pre-Cracked Specimens  $G_C$  versus Zero Treatment Time





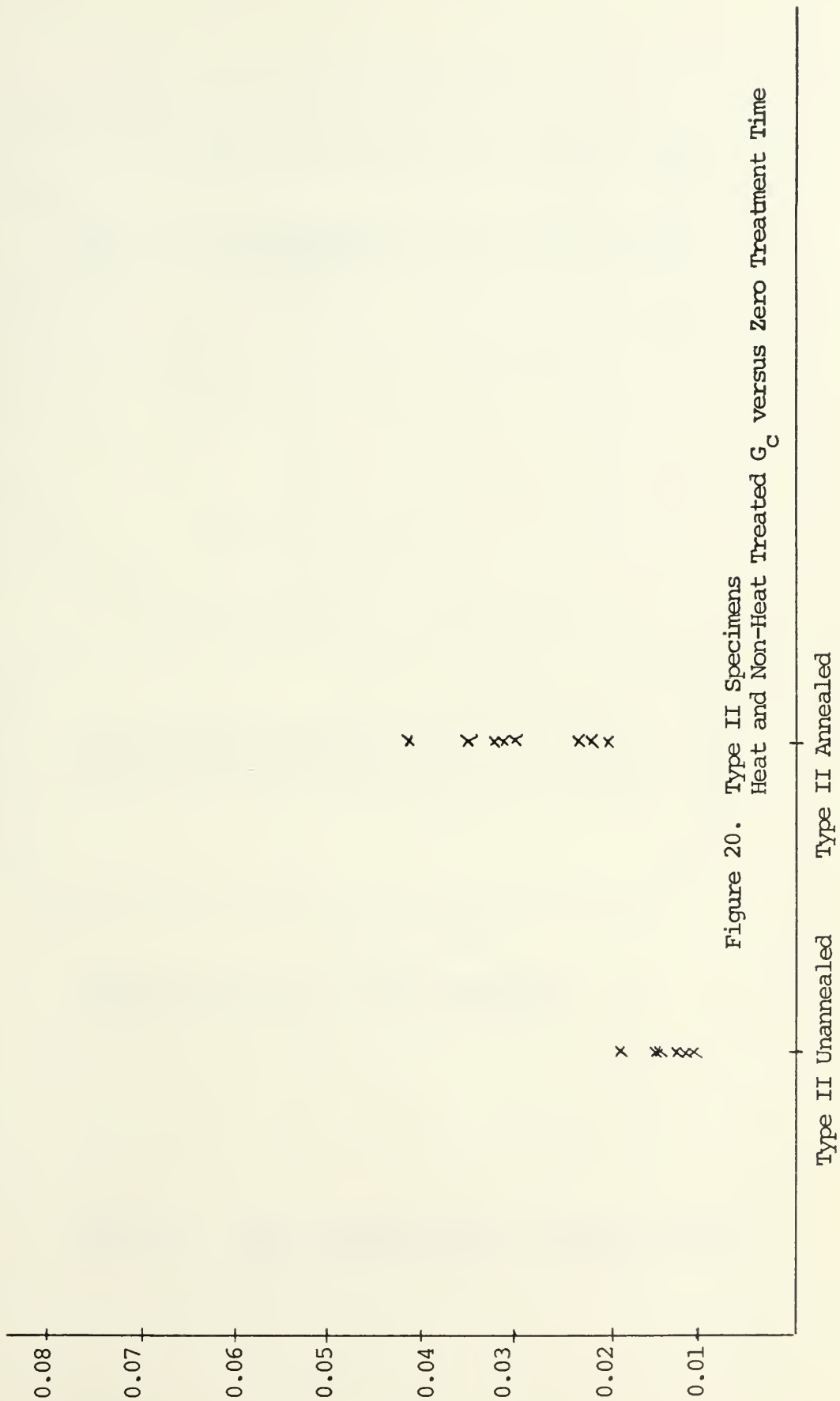
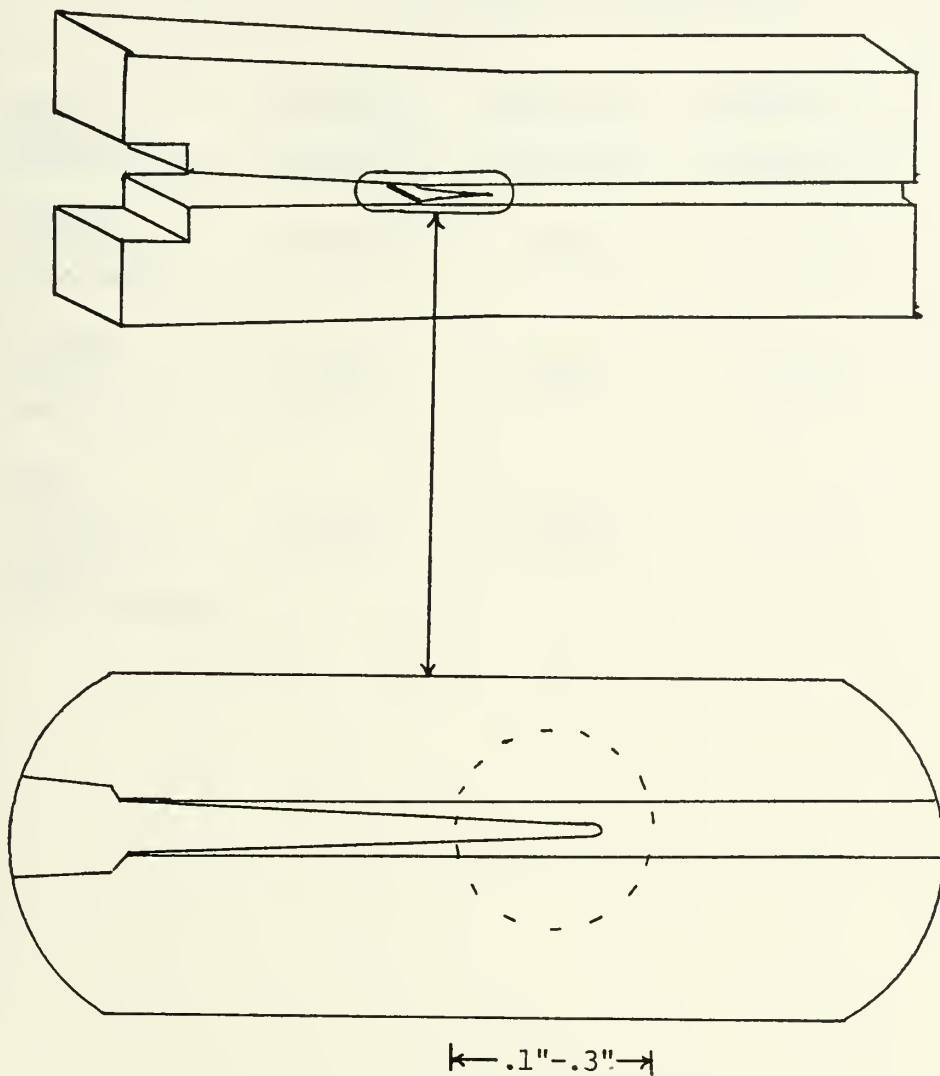


Figure 20. Type II Specimens  
Heat and Non-Heat Treated  $G_c$  versus Zero Treatment Time





Approximate area to which impermeable  
coating was applied is shown circled.

Figure 21. Type I Specimen Used for Special Testing  
Area of Macroflaw Tip is Enlarged



Table VII. Special Type I Specimen  $G_C$ 's

Type of Specimen	Average $G_C$ in-lbf/in <sup>2</sup>	Maximum $G_C$ in-lbf/in <sup>2</sup>	Minimum $G_C$ in-lbf/in <sup>2</sup>
Coated 1/2 hour treatment	0.0216	0.0303	0.0159
Coated 24 hour treatment	0.0314	0.0373	0.0277
Type I 24 hour treatment prior to guide grooves	0.0214	0.0307	0.0158





specimens receiving 24 hour treatments prior to application of guide grooves is similar to that of Type I control specimens. Two interpretations of these data exist. It is possible that diffusion took place primarily along the cracks rather than in from the edges and the specimens receiving guide grooves after treatment failed at flaws generated by their application. Or, the direction of diffusion was in from the flaw edges and the cement was not truly impermeable or was improperly applied. Further experiments to resolve this problem were inconclusive. Figure 22 graphically presents the data resulting from these tests.

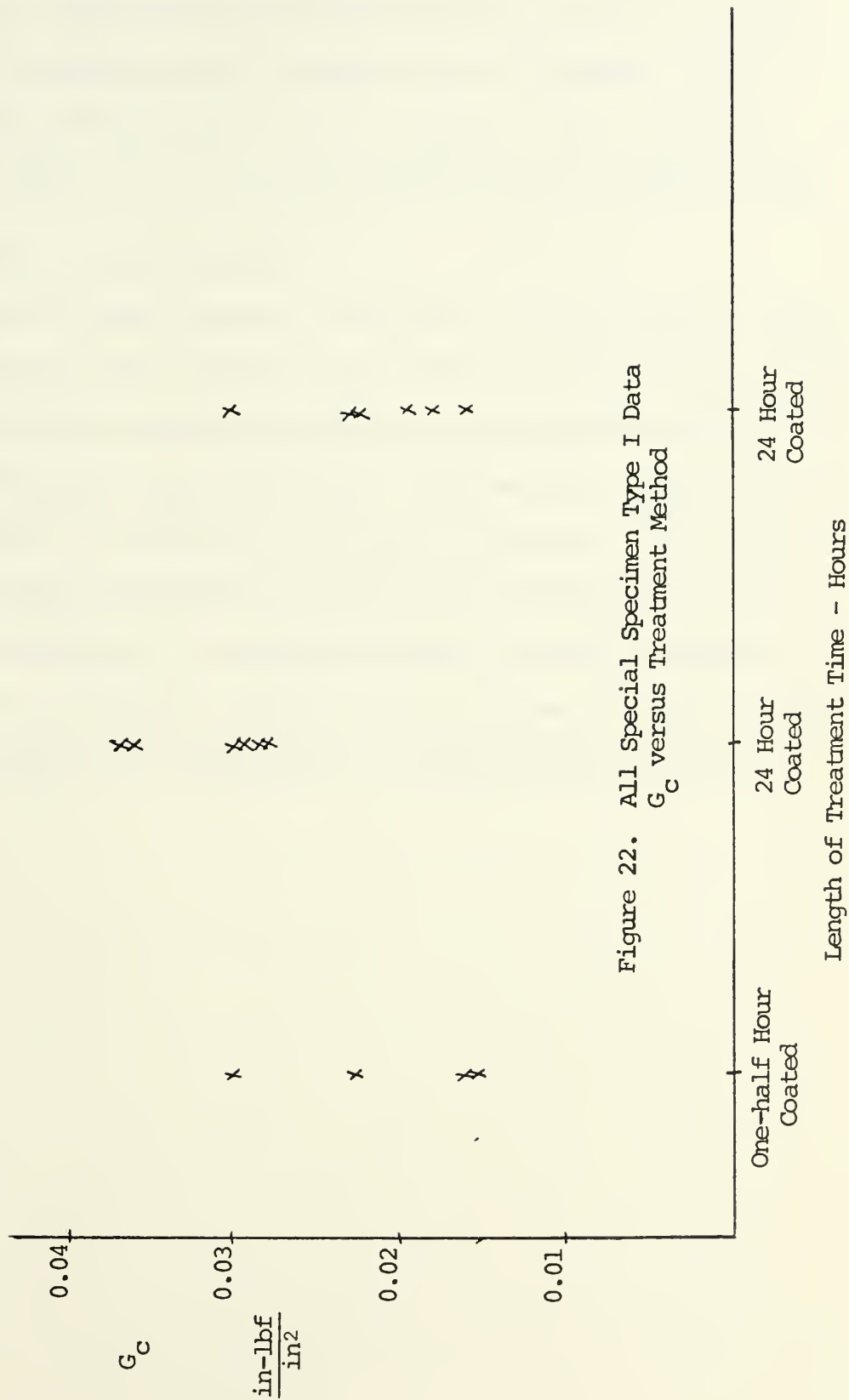
The large values for standard deviations throughout this work are thought to result from several factors. First, the use of thermally blunted macroflaws implies variation in flaw dimensions, particularly crack tip radius. The dependence of the maximum tensile stress near a flaw tip on the crack tip radius is shown in Equation 2.

Secondly, the fracture mechanics analysis used is subject to certain restrictions. They are: (1) the cantilever arms must be of equal and constant height, i.e., the crack must be exactly centered, (2) the crack tip must be perpendicular to its length, and (3) the crack must not veer off from the center. Any discrepancy from these requirements would create variation in the values obtained.

Thirdly, the loading fixtures were not exact knife edges, and the environment and method of loading effected the results. However, the rate of loading was a constant machine factor and chosen high enough to minimize environmental effects.

Fourthly, the variation within the healed regions of the Type I specimens described in Figure 11 created some scatter.







Finally, the inherent inhomogenieties of the glass may have produced some scatter. This brittleness may have made the specimens susceptible to internal discrepancies such as bubbles, pits, or stones.

The above departures from a perfect specimen, crack, and fracture environment explain some of the scatter but not the strengthening noted.

#### D. RELATIONSHIP TO PREVIOUS WORKS

The values of surface energies calculated by various previous investigators are given in Table VIII [1]. The average  $G_c$  obtained for the glass used in this work was converted to surface energy using Equation (5).

(Plastic deformation assumed negligible.) The resultant average value of surface energy,  $\gamma$ , is 0.0110 in-lbf/in<sup>2</sup> or 1.92 Joule/M<sup>2</sup>. This value is of the same order of magnitude as those listed in Table VIII and is in excellent agreement with the results of Shand. An order of magnitude agreement seems reasonable considering the variations of glass composition that are possible and the differences in the experimental procedures.



Table VIII. Fracture Surface Energies of Soda-Lime Glass, Other Studies

Fracture Surface Energy Joule/M <sup>2</sup>	Reference	
3.91	Weiderhorn	N <sub>2</sub> (g) 300°K
4.06	Berdennikov	in vacuum
1.8-10	Roesler	
4-7	Davidge and Tappin	work of fracture method
3.4-5.2	Nakayama	
6-7	Davidge and Tappin	
8-11	Davidge and Tappin	Compliance Method
1.70	Shand	
4.52	Wiederhorn	N <sub>2</sub> (l) - 77°K
4.46*	Liemandt	

Note: All measurements were obtained at room temperature using Griffity-type equations except where otherwise stated.

\*The validity of this value is in doubt.





## VII. RECOMMENDED FURTHER STUDIES

The recent use of massive glass as the partial hull for a deep submersible, the DEEP VIEW, at the Naval Undersea Center, San Diego, California, indicates the amount of new attention being given glass as a structural material for deep submergence oceanographic work. Its use as a man-rated hull makes further work, to gain a better understanding of glass behavior, and to develop non-destructive testing techniques, necessary. Some possible directions of this further work are:

1. The determination of safe working limits of glass structures. A possible technique would entail loading glass structures to failure in a high pressure chamber. A plot of the intensity and pattern of the acoustic emissions prior to failure could be related to the percentage of destructive load.
2. A second technique possible would require similar methods utilizing photoelastic patterns rather than acoustic emissions.
3. A final technique would entail correlation of the previous two.



### VIII. CONCLUSIONS

1. The ion exchange method of chemical tempering can be used to study the strengthening of blunted macroflaws.
2. The critical strain energy release rate,  $G_c$ , for both the thermally blunted and sawcut specimens increased with time when the specimens were treated in the  $KNO_3$  salt bath at  $365^\circ C$ .
3. Thermally blunted specimens exhibited appreciably higher values of  $G_c$  than the non-blunted specimens.



## LIST OF REFERENCES

1. Liemandt, Michael Jerome, A Study of the Effect of the Ion Exchange Method of Chemical Tempering on a Macroflaw in Soda-Lime Glass, Master's Thesis, United States Naval Postgraduate School, Monterey, California, September 1971.
2. Warren, B. E., "X-Ray Determination of the Structure of Liquids and Glass," Journal of Applied Physics, v. 8, p. 645-654, October 1937.
3. Pauling, L., "The Sizes of Ions and the Structure of Ionic Crystals," The Journal of the American Chemical Society, v. 49, p. 771, March 1927.
4. Wiederhorn, S. M., "Environmental Stress Corrosion Cracking of Glass," National Bureau of Standards Report 10565, p. 1-22, April 1971.
5. Burggraaf, S. J., The Mechanical Strength of Alkali-Aluminosilicate Glasses After Ion Exchange, Ph.D. Thesis, Technical University of Eindhoven, Eindhoven, Holland, 21 September 1965.
6. Stookey, S. D., "Strengthening Glass and Glass-Ceramics by Built-In Surface Compression," High Strength Materials, edited by Victor F. Zackay, p. 669-681, John Wiley and Sons, Inc., 1965.
7. Griffith, A. A., "The Phenomena of Rupture and Flow in Solids," Philosophical Transactions of the Royal Society of London, v. A221, p. 163-198, March 1921.
8. Hillig, W. B., and Charles, R. J., "Surfaces, Stress-Dependent Surface Reactions, and Strength," High Strength Materials, edited by Victor F. Zackag, p. 682-705, John Wiley and Sons, Inc., 1965.
9. Gilman, J. J., "Direct Measurement of the Surface Energies of Crystals," Journal of Applied Physics, v. 31, p. 2209, December 1960.
10. Westwood, A. R. C., and Hitch, T. T., "Surface Energy of {100} Potassium Chloride," Journal of Applied Physics, v. 34, p. 3085-3089, 1963.
11. Wiederhorn, S. M., "Fracture Surface Energy of Glass," Journal of the American Ceramic Society, v. 52, p. 99-105, February 1969.
12. Wiederhorn, S. M., "Influence of Water Vapor on Crack Propagation in Soda-Lime Glass," Journal of the American Ceramic Society, v. 50, p. 407-413, August 1967.
13. Wiederhorn, S. M., "Effects of Environment on the Fracture of Glass," Environment-Sensitive Mechanical Behavior of Materials, edited by A. R. C. Westwood and N. S. Stoloff, p. 293-315, Gordon and Breach, New York, 1966.



14. Wiederhorn, S. M., "Fracture Surface Energy of Soda-Lime Glass," Materials Science Research, edited by W. Wurth Kriegel and Hayne Palmour III, v. 3, p. 503-528, Plenum Press, 1966.
15. Wiederhorn, S. M., "Fracture of Ceramics," Mechanical and Thermal Properties of Ceramics, edited by J. B. Wachtman, Jr., p. 217-241, National Bureau of Standards, May 1969.
16. Wiederhorn, S. M., Shorb, A. M., and Moses, R. L., "Critical Analysis of the Theory of the Double Cantilever Method of Measuring Fracture Surface Energies," Journal of Applied Physics, v. 39, p. 1569-1572, 15 February 1968.
17. Ripling, E. J., Mostouog, S., and Patrick, R. L., "Measuring the Fracture Toughness of Adhesive Joints," Materials Research and Standards, v. 4, p. 129-134, March 1964.
18. Naval Research Laboratory Report 1678, Moisture Assisted Slow Crack Extension in Glass Plates, by G. R. Erwin, p. 1-20, 28 January 1966.
19. Wiederhorn, S. M., and Townsend, P. R., "Crack Healing in Glass," Presented at the 72nd Annual Meeting, The American Ceramic Society, Philadelphia, Pennsylvania, May 6, 1970.





# INITIAL DISTRIBUTION LIST

	No. Copies
1. Defense Documentation Center Cameron Station Alexandria, Virginia 22314	2
2. Library, Code 0212 Naval Postgraduate School Monterey, California 93940	2
3. Doctor Ned A. Ostenso Office of Naval Research 480D Arlington, Virginia 22217	1
4. Department of Oceanography, Code 58 Naval Postgraduate School Monterey, California 93940	3
5. Assistant Professor R. B. Leonesio, Code 5416 Department of Material Science and Chemistry Naval Postgraduate School Monterey, California 93940	4
6. Associate Professor J. J. von Schwind, Code 58vs Department of Oceanography Naval Postgraduate School Monterey, California 93940	1
7. LT William R. Burcham 1329 Miles Avenue Pacific Grove, California 93950	2
8. Mr. H. A. Perry Code 2301 Naval Ordnance Lab White Oaks, Maryland 21502	1
9. Oceanographer of the Navy The Madison Building 732 N. Washington Street Alexandria, Virginia 22314	1



UNCLASSIFIED

Security Classification

## DOCUMENT CONTROL DATA - R &amp; D

(Security classification of title, body of abstract and indexing annotation must be entered when the overall report is classified)

1. ORIGINATING ACTIVITY (Corporate author) Naval Postgraduate School Monterey, California 93940		2a. REPORT SECURITY CLASSIFICATION Unclassified	
		2b. GROUP	
3. REPORT TITLE A Study of the Effect of the Ion Exchange Strengthening Method on Macroflaws in Soda-Lime Glass			
4. DESCRIPTIVE NOTES (Type of report and, inclusive dates) Master's Thesis; March 1972			
5. AUTHOR(S) (First name, middle initial, last name) William Richard Burcham			
6. REPORT DATE March 1972	7a. TOTAL NO. OF PAGES 59	7b. NO. OF REFS 19	
8a. CONTRACT OR GRANT NO.		9a. ORIGINATOR'S REPORT NUMBER(S)	
b. PROJECT NO.			
c.		9b. OTHER REPORT NO(S) (Any other numbers that may be assigned this report)	
d.			
10. DISTRIBUTION STATEMENT Approved for public release; distribution unlimited.			
11. SUPPLEMENTARY NOTES		12. SPONSORING MILITARY ACTIVITY Naval Postgraduate School Monterey, California 93940	
13. ABSTRACT			

This work examines the strengthening effect of the ion exchange method of chemical tempering on two specific types of macroflaws, a thermally blunted crack and a sawcut, in soda-lime glass. The use of these macroflaws permitted a quantitative fracture mechanics analysis of the amount of strengthening produced, and a greater access for ion exchange at the flaw tip then could be afforded by a sharp crack. The specimens were treated for various lengths of time in a potassium nitrate bath at 365°C. A double cantilever cleavage technique of measuring fracture surface energy was used to find  $G_C$ , the strain energy release rate. The average increase in  $G_C$  was found to be roughly linear reaching a maximum level of approximately 200% at twelve hours of treatment for the blunted crack specimen type, while a similar maximum of approximately 200% was reached at six hours of treatment for the sawcut specimen type.



KEY WORDS	LINK A		LINK B		LINK C	
	ROLE	WT	ROLE	WT	ROLE	WT
Strengthening of Glass Ion Exchange Tempering of Glass Double Cantilever Cleavage of Glass Glass Tempering and Fracture Macroflow Fracture of Glass Thermal Blunting						

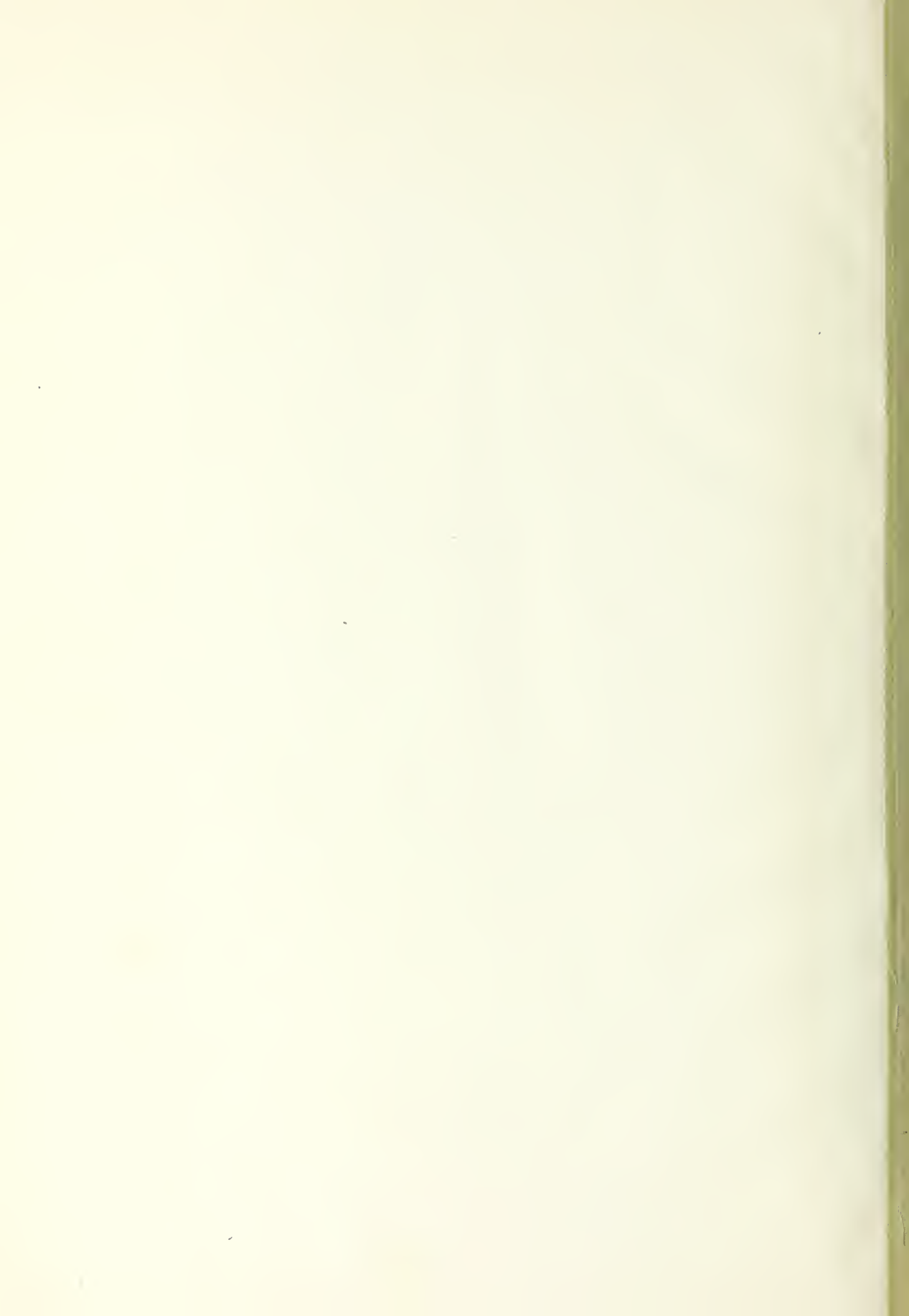












Thesis  
B853  
c.1

Burcham

134037

A study of the effect  
of the ion exchange  
strengthening method on  
macroflaws in soda-lime  
glass.

ct

on

Thesis  
B853  
c.1

Burcham

134037

A study of the effect  
on the ion exchange  
strengthening method on  
macroflaws in soda-lime  
glass.

thesB853

A study of the effect of the ion exchang



3 2768 002 07922 0

DUDLEY KNOX LIBRARY